



HAL
open science

Thirteenth-century stained glass windows of the Sainte-Chapelle in Paris: an insight into medieval glazing work practices

Myrtille O.J.Y. Hunault, Fanny Bauchau, Karine Boulanger, Michel Hérold,
Georges Calas, Quentin Lemasson, Laurent Pichon, Claire Pacheco, Claudine
Loisel

► To cite this version:

Myrtille O.J.Y. Hunault, Fanny Bauchau, Karine Boulanger, Michel Hérold, Georges Calas, et al.. Thirteenth-century stained glass windows of the Sainte-Chapelle in Paris: an insight into medieval glazing work practices. *Journal of Archaeological Science: Reports*, 2021, 35, pp.102753. 10.1016/j.jasrep.2020.102753 . hal-03292392

HAL Id: hal-03292392

<https://hal.sorbonne-universite.fr/hal-03292392>

Submitted on 20 Jul 2021

HAL is a multi-disciplinary open access archive for the deposit and dissemination of scientific research documents, whether they are published or not. The documents may come from teaching and research institutions in France or abroad, or from public or private research centers.

L'archive ouverte pluridisciplinaire **HAL**, est destinée au dépôt et à la diffusion de documents scientifiques de niveau recherche, publiés ou non, émanant des établissements d'enseignement et de recherche français ou étrangers, des laboratoires publics ou privés.

Thirteenth-century stained glass windows of the Sainte-Chapelle in Paris: an insight into medieval glazing work practices

Myrtille O.J.Y. Hunault,^{a,b,d,1} Fanny Bauchau,^{a,b,2} Karine Boulanger,^c Michel Hérold,^c Georges Calas,^d Quentin Lemasson,^{e,f} Laurent Pichon,^{e,f} Claire Pacheco,^{e,f} and Claudine Loisel^{a,b}

^a, Laboratoire de Recherche des Monuments Historiques, Ministère de la Culture, 77400 Champs-sur-Marne, France

^b, Centre de Recherche sur la Conservation (CRC), Muséum National d'Histoire Naturelle, CNRS, Ministère de la Culture, Paris, France

^c, Centre André Chastel, Sorbonne Université, 2 rue Vivienne, 75002 Paris, France

^d Institut de Minéralogie et de Physique des Matériaux et de Cosmochimie, Sorbonne Université, Place Jussieu, 75005 Paris, France

^e, Centre de recherche et de restauration des musées de France, Palais du Louvre, 14 quai François Mitterrand, 75001 Paris, France

^f, New AGLAE FR 3506 – Chimie-Paristech/Ministère de la Culture et de la Communication, Palais du Louvre, 14 Quai F. Mitterrand, Paris 75001, France

¹Present address: Synchrotron SOLEIL, L'Orme des Merisiers, Saint-Aubin, 91192 Gif-sur-Yvette, France ;

²Present address: CICRP 21, rue Guibal, 13003 MARSEILLE, FRANCE

Abstract

The restoration of the four northern windows of the 13th century Sainte-Chapelle in Paris from 2011 to 2014 has offered a unique opportunity to investigate the chemical composition and color of medieval glasses. This impressive corpus, covering a total surface of 660m², was created in a record time of a few years. The glasses from ten selected panels were analyzed using non-destructive and non-invasive techniques, with a specific consideration for the color of the glasses. Ion beam analyses performed at the New AGLAE facility enabled revealing that all ancient glasses are potash type glasses made from plant ashes, likely beech, in agreement with previous results on off-site panels. The multivariate analysis of major and minor elements demonstrates the presence of compositional clusters with a small variability suggesting the identification of bundles of glasses. The coloration of the glasses was measured by optical absorption spectroscopy, using a mobile spectrophotometer over the entire UV-visible-NIR energy range. The color palette is made of six colors assigned to typical medieval recipes. The chromophores of the different glasses are identified by combining the chemical composition, optical absorption spectroscopy and colorimetry. Colorless, yellow and purple glasses arise from the subtle redox equilibrium between manganese and iron. Their reduced usage shows their uncertain production. Blue glasses are colored by Co²⁺ using saffre from the contemporary German mines, green glasses are colored by Cu²⁺ and Fe³⁺ using high concentrations of copper and red glasses are striated glass colored by metallic copper nanoparticles. Glass matrix and chromophores form compositional clusters, which are spread among the panels of the four windows suggesting that the glazing of these four windows was run simultaneously by the same atelier using the same supply of glass.

Keywords

Sainte-Chapelle, glass, color, PIXE, optical absorption, colorimetry, stained glass

1. Introduction

Archaeological and historical glasses provide unique information on the technological development and artistic sensitivities of past societies (Rehren and Freestone, 2015). Some foundations of our modern industrial societies may be found back in the medieval times and contained in the stone walls of the inherited cathedrals. (Musso, 2017; Panofsky, 1946) During the Middle Ages, the rise of Romanesque followed by Gothic architecture introduced a major change: the increasing size of openings in the walls, to be filled by stained glass windows, offered the opportunity to develop the art of glazing, where glass (translucent and colored glass) symbolized divine light. (Grodecki and Brisac, 1984; Lautier and Kurmann-Schwarz, 2010; Pallot-Frossard, 1998) In the mid 12th century, both Abbot Suger and the monk Theophilus praised the beauty and preciousness of colored glasses, which are similar to gems and would suggest the heavenly Jerusalem. (Grodecki, 1976; Hawthorne and Smith, 1979; Panofsky, 1946) The design and the glazing of larger windows might have been possible thanks to the technological improvement of glass production towards efficiency and high productivity. As a result, France has one of the largest heritage of medieval stained glass windows as revealed by its full inventory recently completed by the Corpus Vitrearum.

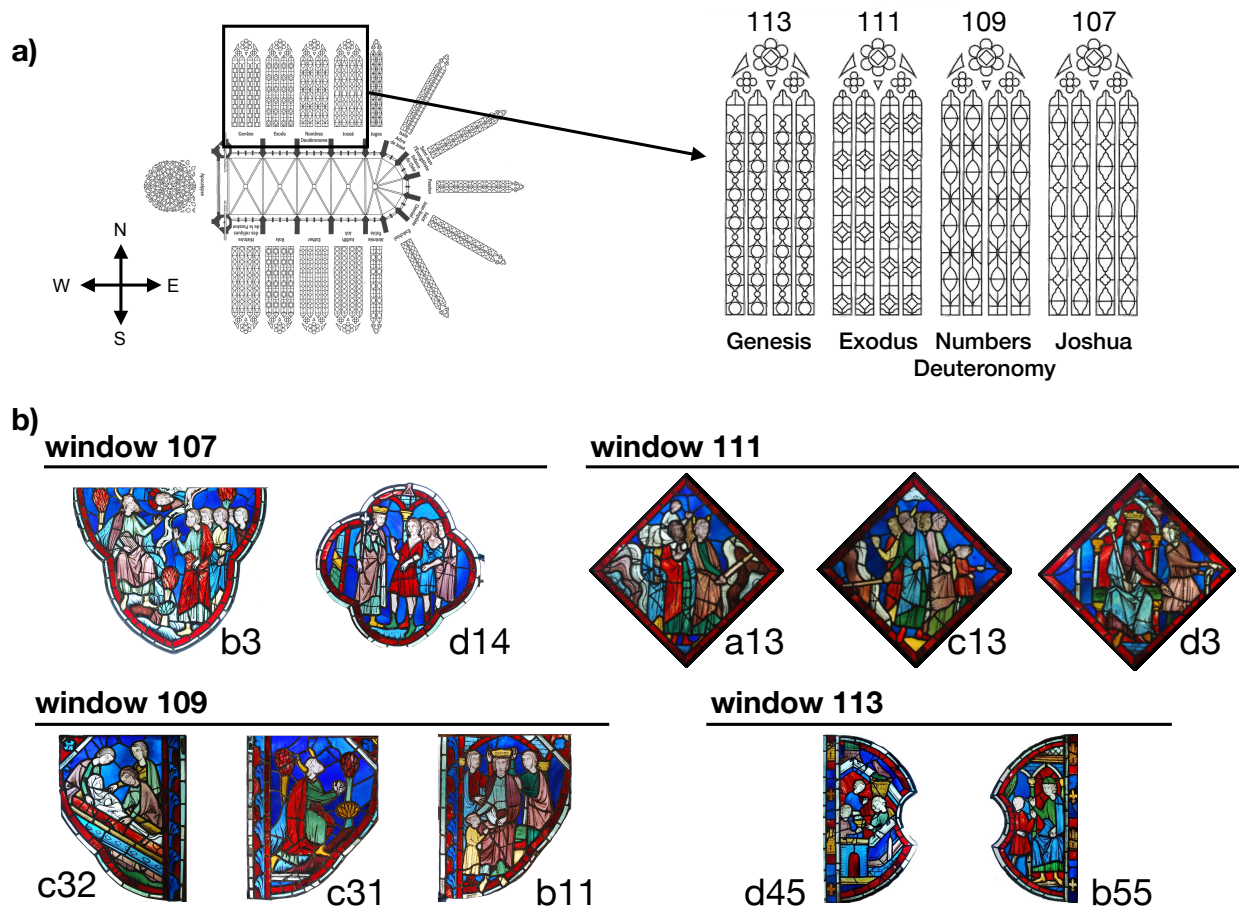
Over one century, the Gothic architectural revolution led to one of the paroxysms of medieval stained glass art: the Sainte Chapelle in Paris, a UNESCO World Heritage Monument, and housing one of the most important corpus of medieval stained glass in the world, described in the first volume of the French Corpus Vitrearum's publications. Built between 1243 and 1248 to receive the relics of the Passion bought by King Louis IX (saint Louis), the exceptional glazing of the upper chapel forms walls of about 660m² of well preserved colored glasses.

The proximity of the images which depict the stories of the Bible, almost reaches saturation of both colors and iconography. (Grodecki and Brisac, 1984) The hundreds of panels assembled in the windows were achieved within the construction time of the Sainte-Chapelle, thus in a span of only 6 years. This impressive efficiency suggests the collaboration of dozens of glaziers from different ateliers to complete the work in such a short time. (Grodecki and Brisac, 1984)

While the details of the work of Abbot Suger in the 12th century in the management of the construction and glazing of the abbey of Saint-Denis, France, are well documented (Panofsky, 1946), few original stained glass panels have been preserved. On the contrary, the Sainte-Chapelle in Paris is a uniquely well-preserved large corpus of stained glass, yet all archives about the construction and its glazing have been lost. Glass chemistry thus provides a precious insight in glass history, medieval glassmaking technology and glazing work organization. The study of the composition and the coloration of glasses is therefore an essential step in our knowledge of this material, its fabrication, and use in medieval times. Yet these glasses remain largely under-studied for only a few panels could be submitted to chemical analysis so far. To our knowledge, the only available chemical composition data published were obtained on panels removed from the building and belonging to museum collections. (Lagabrielle and Velde, 2005; Verita et al., 2005) This previous work led to hypotheses suggesting that the glass used for glazing the windows was provided from two different regions of France: Ile-de-France and Normandy. However, these studies were restricted to a few glass samples and to a limited number of chemical elements. The opportunity of the restoration in 2011-2014 of the northern stained glass windows granted access to ten panels from windows 107, 109, 111, and 113 for non-destructive chemical, spectroscopic and colorimetric characterization providing for the first time a large scale investigation of these glasses.

The chemical composition was obtained on 110 glasses from the ten panels by ion-beam analytical (IBA) methods, which allows the characterization of a large set of 35 major and trace chemical elements in a single acquisition. (Calligaro, 2008; Fleming and Swann, 1987; Hunault et al., 2017a; Kuisma-Kursula, 2000; Van Wersch et al., 2016; Vilarigues et al., 2019; Vilarigues and da Silva, 2004) The colors of the five panels of windows 111 and 113 were also investigated by optical

102 absorption spectroscopy using a portable optical spectrometer developed for contactless
 103 measurements(Hunault et al., 2016b). The glasses were studied after their restoration, thus
 104 allowing the reduction of the effect of surface deposit on the measurements. The handling of the
 105 complete panels allowed us to select the significant glasses to be analyzed from aesthetical,
 106 historical and chemical points of view.
 107 We first report the chemical composition study of the glass matrix and its interpretation in terms of
 108 origin and glass recipes based on a multivariate analysis. We discuss the variability and dispersion
 109 of element concentration as a proxy of the glasshouse provenance. Then we describe the recipe of
 110 each glass color. Colorless, purple and yellow colors are first described together as they arise from
 111 subtle redox equilibria between iron and manganese ions as found in the monk Theophilus' treatise
 112 (Royce-Roll, 1994; Schreurs and Brill, 1984; Sellner et al., 1979; Theophilus, 1847). Blue, green
 113 and red colors are obtained by the addition of cobalt or copper. The sources for these elements are
 114 inferred and discussed.



115
 116 **Figure 1:** a) The four windows restored in 2011-2014 and their location in the Sainte-Chapelle in Paris. b) The 10 analyzed
 117 panels.

118
 119 **2. Methods**

120 **2.1. Historical identification of the glasses**

121 The 15.5m-high windows of the nave, composed of thin lancets and crowned by small roses, were
 122 assembled from hundreds of small panels, covering a total surface of 660m². The careful study of
 123 the windows by art historians both in the 1950's and during the last restoration revealed that most
 124 of the glasses date from the 13th century,(Aubert et al., 1959; Grodecki and Brisac, 1984) thus
 125 providing an exceptional corpus of glasses testifying of the medieval glassmaking techniques. ,
 126 The windows of the nave follow a complex iconographic program.(Aubert et al., 1959) The style of
 127 these stained glass windows is characterized by a simplification of the lines tending toward
 128 elegance. The color palette used is composed of red, blue, purple, green, yellow and colorless
 129 glass, the red and blue colors dominating the overall effect created by this colorful pattern. The

130 stained glass windows of the nave are attributed to three glazing ateliers based on the differences
131 between the style of the painting.(Grodecki and Brisac, 1984)
132 Over centuries, they underwent several modifications, including the removal of numerous panels
133 located in the lower part of the windows at the end of the 18th century and the beginning of the 19th
134 century, when the building was used to accommodate the archives.(Grodecki and Brisac, 1984;
135 Loisel, 2020) Some panels have been lost, while others are now in museum collections in France,
136 Great-Britain and the USA.(Smith, 2015) An important restoration campaign decided by King Louis-
137 Philippe in 1837 and undertaken between 1848 and 1855 resulted in the completion of the stained
138 glass windows, by the means of new stained glass panels carefully imitating the remaining
139 medieval ones.(Aubert et al., 1959)
140 The ten studied panels were observed by naked eye to achieve a critical identification of each
141 glass pieces. The dating was achieved using several criteria: color, marks of blowing technique,
142 irregularities, relative thickness variations, cutting pattern of the edges when visible, alterations and
143 eventually the paintings on the glasses. It enabled to distinguish original glasses from the 13th
144 century and more recent glasses introduced during the successive restoration campaigns.
145 During the restoration of 2011-2014, ten panels from the North side, the windows of Joshua,
146 (window 107), Numbers and Deuteronomy (w. 109), Exodus (w. 111) and Genesis (w. 113) (Figure
147 1) were studied. According to stylistic analyses these four windows were glazed by the same artist
148 from the main glazing atelier.(Grodecki and Brisac, 1984)
149

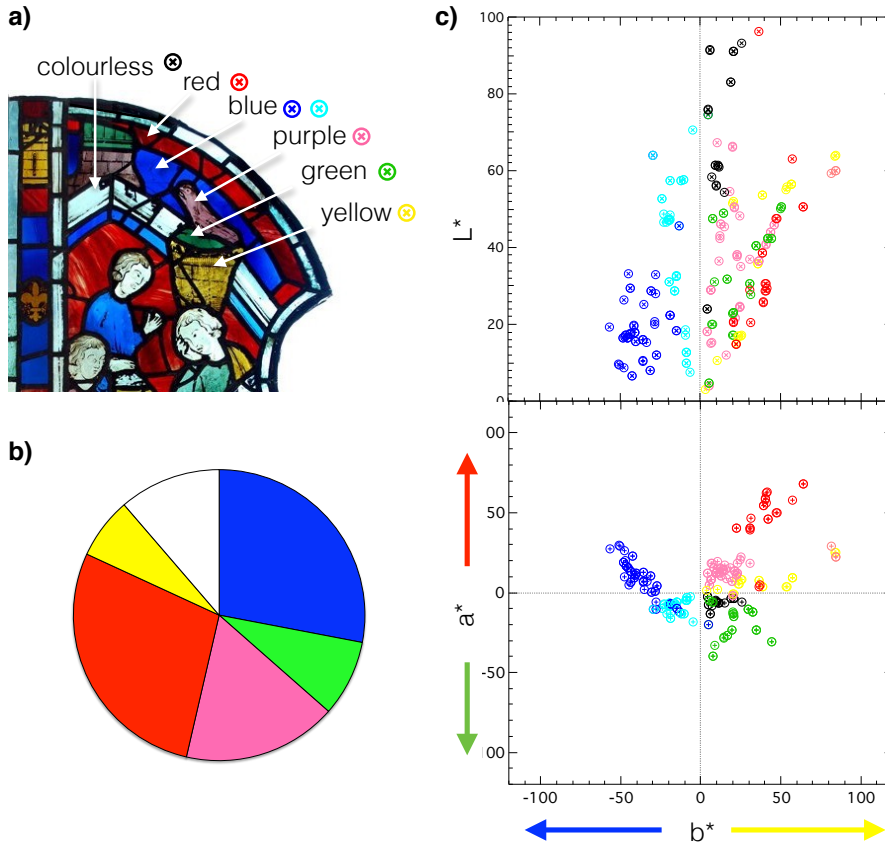
150 2.2. PIXE-PIGE chemical composition analysis

151 A total of 110 glasses were analyzed by Particle Induced X-ray Emission and Particle Induced
152 Gamma Emission (PIXE and PIGE) techniques at the new AGLAE facility of the C2RMF in the
153 Louvre (Paris, France).(Pichon et al., 2014) These non-destructive analyses were performed
154 directly on the panels without sampling or removing the glass pieces. The repartition of the
155 analyzed samples between the windows and the colors is given in supporting information (SI).
156 PIXE and PIGE analyses were performed simultaneously. PIXE analysis was performed using
157 four SDD detectors: the first one was dedicated to the analysis of low Z elements ($10 < Z < 29$)
158 and a helium flux was used to reduce the absorption of incident and remitted beams by air;
159 the three other SDD detectors were dedicated to high Z elements ($Z > 26$) and an aluminum
160 filter ($50\mu\text{m}$ -thick) was placed in front of the detector in order to absorb the low energy X-rays.
161 One HPGe detector was used for PIGE measurements. The incident proton beam was 3 MeV
162 with an intensity of 3 to 4 nA. The chemical composition was averaged over an analyzed area
163 of $1000\mu\text{m} \times 1000\mu\text{m}$, using a $50\mu\text{m}$ -diameter beam. For each glass sample, three
164 measurements were performed at different points. The obtained compositions correspond to
165 the mean composition of all the analyzed area. The analyses were performed on the inner
166 side of the panels, less altered, after cleaning the analyzed area with a water-ethanol solution.
167 The PIXE spectra were extracted using GUPIX software combined with TRAUPIXE software
168 developed at AGLAE(Pichon et al., 2015), assuming that analyzed zones were homogeneous
169 and that all elements were present as oxides. The geochemical diorite DR-N sample and Brill
170 glasses were used as reference material to calibrate the PIGE data and control PIXE results.
171 The compositions given in this paper result from the combination of PIXE data and the sodium
172 content obtained by PIGE.
173 Data were analyzed using the R software. Hierarchical cluster analysis (HCA) was performed
174 after renormalization using Ward's method and Euclidean distances (see SI). This data
175 analysis tool has been used previously in several studies of ancient glasses to compare glass
176 compositions.(Cox and Gillies, 1986; Kunicki-Goldfinger et al., 2000; Schalm et al., 2007)
177

178 2.3. Optical absorption spectroscopy

179 The optical absorption spectroscopy measurements were performed in parallel to the chemical
180 analysis on the same glass pieces. We used a mobile setup described elsewhere,(Hunault et
181 al., 2016b) which enabled to measure optical absorption spectra in transmission over the
182 entire UV-visible-NIR energy range (350-2500 nm). The beam size on the sample was smaller
183 than 1 mm^2 and enabled to select a precise spot of analysis, free from alteration and paint.

184 Colorimetric analyses were achieved by computing the CIE L*a*b* values (unit less) in the
 185 colorimetric system defined in 1976 by the International Commission on Illumination. The
 186 colorimetric CIE L*a*b* values were calculated using D65 illuminant and CIE 1931 2° observer. L*
 187 describes the luminosity of the color (0: black; 100: white) and a* and b* describes the color hue:
 188 a* varies from -120 (green) to 120 (red) and b* varies from -120 (blue) to 120 (yellow), the higher
 189 a* and b* in absolute value, the more saturated the color.
 190



191
 192 **Figure 2:** a) Detail of the panel d45 (w. 113) and identification of the colors; b) Average glass surface fraction per color
 193 obtained for the ten panels of this study; c) CIE L*a*b* parameters obtained from optical absorption spectroscopy.

194
 195

3. Results and interpretations

3.1. Dating of the investigated panels

196
 197
 198
 199 The ten panels of windows 107, 109, 111 and 113 that have been analyzed by portable optical
 200 absorption spectroscopy and PIXE-PIGE analysis are presented in Figure 1 and the corresponding
 201 restoration charts provided in Supporting information (SI) confirm that the majority of the glasses
 202 were original. The artistic and material quality of these windows is well preserved, despite the fact
 203 that these 13th century glasses have been altered by the atmosphere and air (Godoi et al., 2006;
 204 Bernardi et al., 2013). This study focuses on the original glasses from the 13th century
 205 representative of the different colors present in the four windows.
 206

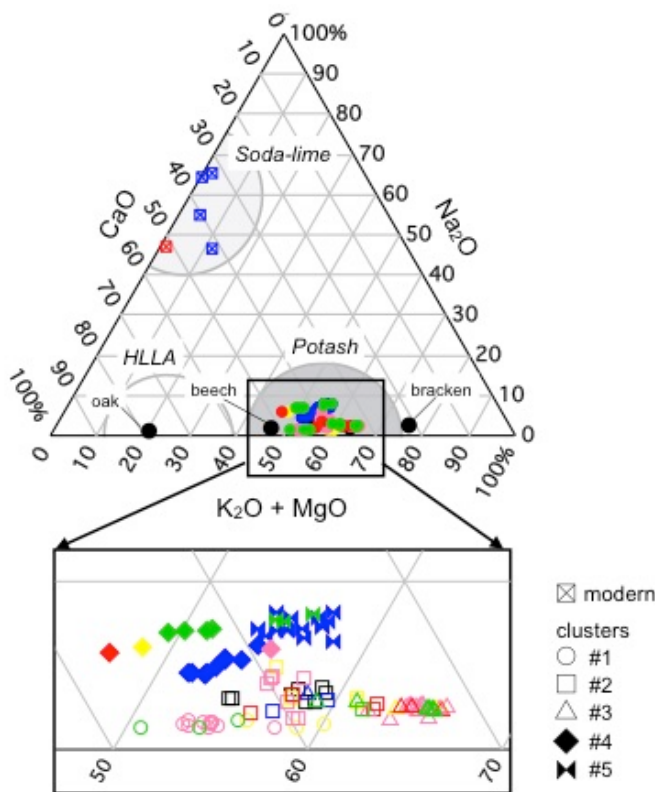
3.2. The color palette

207
 208 Medieval stained glass windows are well known for the diversity of their colors. The colors of the
 209 glasses are named according to the usual terminology used by art historians: yellow, purple, red,
 210 blue, green, and colorless glasses (Figure 2a). This color distinction will be used hereinafter to
 211 report and discuss the chemical composition, spectroscopic and colorimetric data. By “colorless”
 212 we refer to glass that is not remarkably colored, either with a residual “natural” color or decolorized

213 by the addition of specific chemical elements. Other authors use the word “white” instead of
 214 “colorless” (Bidegaray et al., 2020; Gliozzo, 2016; Jackson, 2005).
 215 Figure 2b shows the fraction of glazed surfaces of each color averaged by image analysis using
 216 GIMP software, over the ten studied panels. Blue and red glasses are the dominating colors in
 217 terms of surface, which confirms the general blue-and-red visual impression created by these
 218 stained glass windows. Based on the estimate of the total surface of 660 m² of the glazing of the
 219 nave windows, this gives a surface of 185 m² for red and blue glasses and 110 m² for purple
 220 glasses. Other colors correspond to a more limited surface: 70 m² for colorless glass and 60 and
 221 45 m² for green and yellow glasses, respectively.
 222

223 The 1976 CIELAB color space coordinates (L*, a*, b*) provide a way to quantify the variability of
 224 the hue and luminance. Figure 2c presents the colorimetric parameters of the studied glasses for
 225 each color. Red glass is the most saturated color with high absolute a* and b* values. The blue
 226 glasses split into two groups, according to a* value: negative or positive for the greenish or reddish
 227 hue, respectively. These two colors span over a wide range of a* and b* values together with green
 228 glasses and yellow glasses. Purple and colorless glasses consist of a more reduced range of a*
 229 and b* values. The glasses cover the entire range of luminance values L*, and we can note that
 230 blue glasses are generally darker (lower L* value) than colorless glasses (higher L* value).
 231 Color results from the overall absorption of light by the material, thus not only the chromophores,
 232 added to the glass to give its color but also surface alteration or paint influence the color. Although
 233 we took special care to analyze glasses with minimal influence of alteration and paint, the variation
 234 in luminance L* value may reflect the influence from both factors.
 235 In the followings, we will use the color distinction described above to report and discuss the
 236 chemical composition data.
 237

238 3.3. Composition of the glass matrix



240 **Figure 3:** Ternary diagram Na₂O-K₂O+MgO-CaO showing the relative concentrations of four major elements characteristic from
 241 the type of flux used to produce the medieval glasses of the Sainte-Chapelle in Paris. The color of the markers represents
 242 the color of the glass in agreement with the colorimetry analysis (see main text). The inset shows the distinction between
 243 the five clusters of compositions found within the “potash” group using hierarchical cluster analysis (see main text);
 244

245 *Chemical compositions of glasses obtained from specific ashes from ref.(Jackson and Smedley, 2004), are indicated (black*
246 *full circles).*

247

248 3.3.1. Medieval recipe: wood-ash glasses

249 • Glass type

250 Medieval glasses were obtained by melting together silica from sand and a flux. The chemical
251 composition of the resulting glass reveals to some extent the nature of the flux used. Compositions
252 of ancient glasses from the 12th-16th centuries have been classified by several authors (Adlington
253 and Freestone, 2017; Gratuze, 2013; Kunicki-Goldfinger et al., 2014; Schalm et al., 2004) into:

254 - "Soda-lime" glasses including natron glasses and halophilic plant ash glasses;

255 - "Potash" glasses: potash-lime silicate glasses obtained using plant ashes;

256 - "High Lime-Low Alkali" (HLLA) glasses: these glasses, obtained using plant ashes, contain more
257 calcium than alkaline elements.

258 The complete set of chemical concentrations of all elements analyzed by PIXE-PIGE at AGLAE
259 can be found as Supporting Information. Figure 3 presents the ternary diagram of the relative
260 concentrations of the four major elements characteristic from the type of flux used to produce the
261 glasses: Na₂O, K₂O, CaO and MgO. Potassium and magnesium are summed together as both
262 come from plant ashes that could have been used as a source of flux.(Jackson et al., 2005;
263 Jackson and Smedley, 2008; Smedley and Jackson, 2002) On the ternary diagram, we have
264 represented the areas for each glass type.

265 Among the 110 analyzed glasses, five glasses originally identified as ancient glasses, were found
266 to be soda-lime glasses with their Na₂O content higher than 11wt%. These glasses were identified
267 as restorations from the 19th century. This is supported by their low magnesium and phosphorous
268 contents, both elements that indicate the use of plant ashes (Jackson et al., 2005; Jackson and
269 Smedley, 2008; Smedley and Jackson, 2002) and by the low impurity level resulting from the use
270 of relatively pure raw materials. *In the following, these glasses will be ignored.*

271 All the 105 other glasses from the ten analyzed panels from the Sainte-Chapelle in Paris belong to
272 the "potash" type area and show high potassium oxide and lime contents (Figure 4a). The high
273 magnesia and phosphate contents further confirm the use of wood ashes (Figure 4b and Figure
274 S5). We note that the glasses from the Sainte-Chapelle in Paris belong to the category of low-lime
275 high-magnesia content (LLHM) as distinguished by Adlington et al. (Adlington et al., 2019) (Figure
276 S5). The phosphate content (in the 3-5wt.% range) and the sodium oxide content are relatively
277 high compared to other plant-ash medieval glasses (Figure S5). Altogether, the composition of the
278 glasses from the Sainte-Chapelle in Paris agrees with the general pattern found for North Western
279 France glasses as reviewed by Adlington et al. (Figure S5). Additionally we note that the chemical
280 composition of the 13th century glasses of the Sainte-Chapelle is similar to several other medieval
281 glasses in terms of potassium oxide, lime, magnesia and phosphate contents: i) earlier glass
282 compositions from the end of the 8th century eastern France.(Van Wersch et al., 2016); ii) 12th
283 century potash glasses from York Minster, UK.(Cox and Gillies, 1986) iii) medieval German wood-
284 ash glasses from before 1400.(Wedepohl and Simon, 2010) and iv) later 15th century Belgian
285 glasses.(Schalm et al., 2007)

286

287 The use of wood ashes as flux agrees with ancient treaties.(Smedley and Jackson, 2002) The
288 fluxing properties of the ashes arise from their alkali and alkaline-earth contents. Depending of the
289 nature of the ashes used in the glass recipe, various chemical compositions were obtained.
290 Despite similar potassium oxide and lime compositions (Figure 4a), the ternary diagram highlights
291 the horizontal spread of the data along the CaO-K₂O+MgO joint as well as several distinct Na₂O
292 contents, which can be markers of glass recipe variations.

293

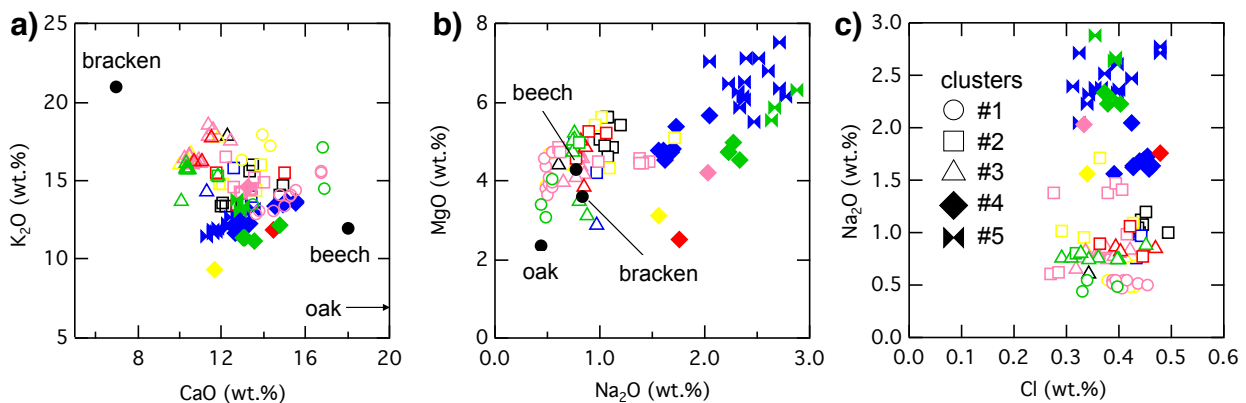
294 • The recipe

295 Experimental studies on the relation between the nature of the ashes and the resulting glass
296 composition are difficult as the composition of wood ashes depends on many factors. Yet previous

297 investigations have brought precious information on the influence of the type of ashes on the final
 298 glass composition. Jackson et al. compared glasses obtained from beech, oak and bracken
 299 ashes.(Jackson and Smedley, 2004) They showed that beech ashes give close K_2O and CaO
 300 contents and high phosphate content; oak ashes give high CaO and low K_2O contents and low
 301 phosphate content; and bracken ashes give high K_2O and low CaO contents and a medium
 302 phosphate content. These compositions are reported in Figures 3 and 4 and S5 for comparison
 303 with the present data. Figure 3 clearly suggests the dominant use of beech ashes potentially mixed
 304 with bracken ashes. (Jackson and Smedley, 2008, 2004; Smedley and Jackson, 2002) Stern and
 305 Geber investigated the chemical composition of glasses made from two different recipes:(Stern
 306 and Gerber, 2004) i) beech ashes and sand and ii) leached beech ashes, potash extract and sand.
 307 The “potash”-type chemical composition found in the present study with close K_2O and CaO
 308 contents is close to the second recipe suggesting the additional use of potash extract obtained
 309 from leached ashes. This is partly in contradiction with the results of the study of Jackson et al.
 310 who used unpurified ashes. However, the second recipe from Stern and Geber’s study does not
 311 account for the high phosphate content. The addition of bracken ashes may explain the observed
 312 high phosphate content. Altogether, the chemical composition of the glasses suggests that the
 313 glasshouses, which provided the glasses for the Sainte-Chapelle, used beech ashes, possibly
 314 mixed with bracken ashes, conforming to the recipe found in the monk Theophilus’
 315 treatise.(Hawthorne and Smith, 1979)

316 The glasses from the Sainte-Chapelle in Paris appear to have among the highest silica content in
 317 Medieval Europe, with an average 57.6 wt% SiO_2 (Figure 3b and see Table I), which is higher than
 318 the values reported in other medieval “potash”-type glasses (Calligaro, 2008; Freestone, 1992;
 319 Hunault et al., 2016a). In their experimental work, Smedley et al. (Smedley et al., 1998), discussed
 320 the weight ratios between ashes and sand according to the monk Theophilus’s treaties, in relation
 321 with the melting temperature of the glass as well as its durability. The higher the ash content, the
 322 lower the melting temperature and the easier the completion of the melt yet resulting in a less
 323 durable final glass. At fixed sand-to-ash ratio, depending on the flux chemical composition, the
 324 resulting melting and working properties of the glass may differ. Vice versa, the sand-to-ash ratio
 325 might have been adjusted depending on the flux composition to obtain similar melting and working
 326 properties of the glass.(Hunault et al., 2017b) Here, the relatively high silica content would suggest
 327 the use of high quality, high durability glass in accordance with the final purpose of the Sainte-
 328 Chapelle building to host the Passion relics.

329
330



331
332
333
334

Figure 4: Chemical compositions analyzed by PIXE-PIGE at the New AGLAE facility a) K_2O vs CaO , b) MgO vs Na_2O and c) Na_2O vs Cl . Markers correspond to the clusters and colors to the glass colors. Error bars are of the size of the markers.

335 • Sodium-enriched potash glasses

336 A number of “potash” type glasses are enriched in sodium (>1.5wt.% Na_2O) (Figure 3 and Figure
 337 4b). A majority of these glasses corresponds to blue glasses, other to some green glasses, and a
 338 few correspond to other colors. The glasses are enriched in both sodium and magnesium, which
 339 discards a possible recycling of natron-based glasses that do not contain magnesium.(Phelps et
 340 al., 2016; Tite et al., 2006) There is no correlation between the chlorine and the sodium contents

341 (Figure 4c): the Cl content is constant in the 0.3-0.5% range, while the Na₂O content varies by a
342 factor of 6. This supports that salt was not used similarly to other medieval Belgian
343 glasses.(Schalm et al., 2007) Furthermore, none of the laboratory synthesized wood ash glasses
344 contain sodium up to similar ranges as observed here (Figure 4b).(Jackson et al., 2005; Jackson
345 and Smedley, 2008; Smedley and Jackson, 2002; Stern and Gerber, 2004) It is therefore not clear
346 whether this sodium increase is related to the nature of the wood ashes.

347 Is the sodium-enrichment a marker from a specific geographical provenance? Sodium-enriched
348 glasses have been found in various medieval glasses (Adlington et al., 2019), such as panels from
349 other windows of the Sainte-Chapelle in Paris (Lagabrielle and Velde, 2005; Verita et al., 2005),
350 from the abbey of Saint-Denis, France (Calligaro, 2008), and from Westminster, UK and Cluny,
351 France.(Freestone, 1992) Based on the comparison with the chemical composition of other French
352 glasses from the same period and in particular the glasses from the cathedral of Rouen, France,
353 previous authors have further hypothesized that the low Na₂O/MgO ratio glasses came from Ile-de-
354 France, France and the high magnesium and sodium content glasses came from Normandy,
355 France.

356 What is the origin of this sodium-enrichment? Little inferences have been made so far. We may
357 suggest two possibilities: i) the recycling of ancient soda-type glasses as was available in Europe
358 until the 12th century (Cox and Gillies, 1986) in low proportions such as significant characteristic
359 impurities are not detected (Bidegaray and Pollard, 2018) or ii) use of sodium-rich seaweed ashes
360 in addition to wood ashes (Adlington et al., 2019; Tite et al., 2006; Wedepohl et al., 2011a).

361 Although the majority of blue glasses found in this study would suggest a specific trade from a
362 distinct glasshouse for this color, or a specific recipe related to the cobalt source(Bidegaray and
363 Pollard, 2018), previous data from other panels from the Sainte-Chapelle, revealed the presence of
364 glasses of similar sodium content with other colors (see Figure S10 in SI). The observation of a
365 similar composition pattern among the different windows suggests that the different glaziers used
366 glass from the same stock.
367

368 3.3.2. Variability of major and trace elements: different 369 glasshouses?

370 The obtained relatively close chemical compositions can suggest a common origin of the glasses.
371 However, some subtle variations are observed. These variations could account for different
372 production origins or variability in the production of one same glasshouse. How close are the
373 chemical compositions of glasses produced in the same glasshouse?

374 Several factors influence the chemical composition of Medieval glasses, independently of the use
375 of coloring additives. The variability within one glasshouse can be separated into “natural” and
376 “behavioral” variations, related to the raw material chemistry and glassmaking techniques,
377 respectively.(Freestone et al., 2009; Jackson et al., 2005) Another factor influencing the chemical
378 composition variation is the time scale over which the compared glasses have been produced in
379 one glasshouse. Indeed, the incidence of “behavioral” and “natural” variations are more likely to be
380 effective over weeks, months and even years than over one single day since glass pots were used
381 over several days.(Freestone et al., 2009) In a recent work, we have estimated the “daily variation”
382 criterion based on the comparison of the chemical composition of four different glasses assembled
383 together in one pane of glass, guarantying that these glasses originated from glass pots operated
384 on the same day.(Hunault et al., 2017a) This criterion corresponds to the variation of glass
385 composition between different glass pots prepared in the same time frame in the same
386 glasshouse. The time unit of one day is supported by the time reference found in Theophilus’
387 treatise, which states that glass could be melted overnight and that it would take only a few hours
388 to observe color changes.(Hawthorne and Smith, 1979; Smedley et al., 1998) We may consider
389 this variation as a reference minimum variation of the production of a glass glasshouse.

390 This “daily variability” criterion can be compared to the composition variation (relative standard
391 deviation) calculated for the major components of all the analyzed ancient glasses of the Sainte-
392 Chapelle in Paris (Table I). We find that the composition variation of the ancient glasses is at least
393 twice larger (for Al₂O₃ and CaO) than the “daily variability”. This agrees with the fact that all the

394 glasses could not be produced over one day in one glasshouse. Hence, the larger variability in the
 395 chemical composition can be assigned to both “natural variability” and “behavioral variability”
 396 across time within the same glasshouse or to different provenances.
 397

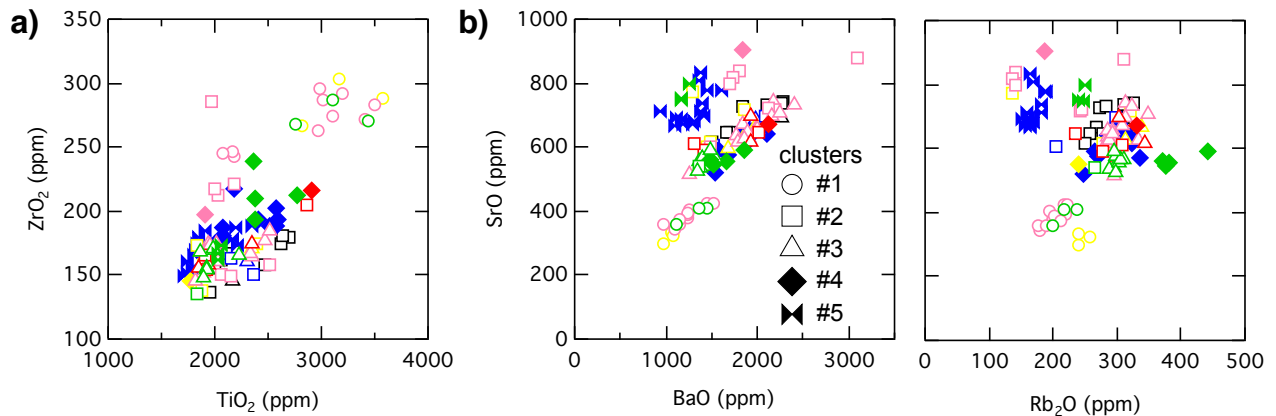
398 Yet according to the ternary and binary diagrams (Figure 3 and Figure 4), it is tempting to define
 399 clusters of data with close chemical compositions. To define clusters of glasses based on more
 400 than two or three chemical composition variables, we used hierarchical cluster analysis (HCA)
 401 considering 13 major and trace elements corresponding to the raw materials of the glass: Si, Na,
 402 K, Ca, Mg, Al, Cl, P, Ti, Rb, Sr, Zr and Ba as oxides. These elements describe the glass batch
 403 independently from coloring chemical elements and other associated elements. Iron and
 404 manganese are excluded from the HCA because their content is also influenced by the addition of
 405 coloring ores (see below).
 406

407 **Table 1** : Average values and relative standard deviation (compositional variability) of chemical composition for the ancient glass
 408 corpus for each cluster.
 409

	Na₂O	MgO	Al₂O₃	SiO₂	P₂O₅	K₂O	CaO
Daily glasshouse variability according to Hunault et al. 2017							
<i>Rel. SD (%)</i>	14	4	6	1	3	4	7
All ancient glasses (N=105)							
<i>Av. (wt%)</i>	1.24	4.84	1.95	57.0	3.97	14.5	12.7
<i>Rel. SD (%)</i>	57	19	11	4	14	13	13
Cluster #1 (N=16)							
<i>Av. (wt%)</i>	0.5	4.0	2.2	54.8	4.9	14.8	15.0
<i>Rel. SD (%)</i>	6.5	12	6.0	4.5	3.5	11.	8.6
Cluster #2 (N=26)							
<i>Av. (wt%)</i>	1.0	4.9	1.8	57.3	3.7	14.7	13
<i>Rel. SD (%)</i>	25	8.7	11	2.9	15	6.1	7.3
Cluster #3 (N=30)							
<i>Av. (wt%)</i>	0.79	4.5	1.8	58.3	3.6	16.4	10.9
<i>Rel. SD (%)</i>	8.5	13	4.8	2.2	5.9	6.6	6.0
Cluster #4 (N=16)							
<i>Av. (wt%)</i>	1.9	4.5	1.9	57.0	4.2	12.4	13.8
<i>Rel. SD (%)</i>	15	17	6.5	5.2	8.3	11	8.3
Cluster #5 (N=17)							
<i>Av. (wt%)</i>	2.5	6.4	2.1	56.0	4.0	12.5	12.4
<i>Rel. SD (%)</i>	8.8	8.9	6.6	2.9	6.5	5.3	5.3

410
 411
 412 The obtained dendrogram and the inertia plot are provided in SI and the significance of the chosen
 413 method is further discussed in the SI and below. The dendrogram first splits into two branches that
 414 mainly correspond to the high and low Na₂O contents respectively and accordingly to most of the
 415 blue glasses and the others. This agrees with the trend observed in the ternary diagram (Figure 3)
 416 and in Figure 4, where two main groups of glasses are separated according to their Na₂O content.
 417 Following the inertia plot we define five significant clusters. The clusters are further described in the
 418 SI. These clusters, based on these 13 major and trace elements, are reported in all plots as
 419 different markers, and agree fairly with the groups of data qualitatively observed in the ternary
 420 diagram and the other binary diagrams (Figure 3 and Figure 4 and hereinafter). In Table I, the
 421 means and relative standard deviations for each cluster are given. We find that the chemical
 422 composition variations for each cluster are very close to the “daily variability”. The narrowest

423 variations are found for cluster #5. Then cluster #3, though the largest one (30 glasses), shows
424 also a low variability.
425
426



427 **Figure 5: Chemical compositions analyzed by PIXE-PIGE at the New AGLAE facility a) ZrO_2 vs TiO_2 ; b) SrO vs. BaO**
428 **and Rb_2O and ; Markers correspond to the clusters. Error bars are of the size of the markers**
429

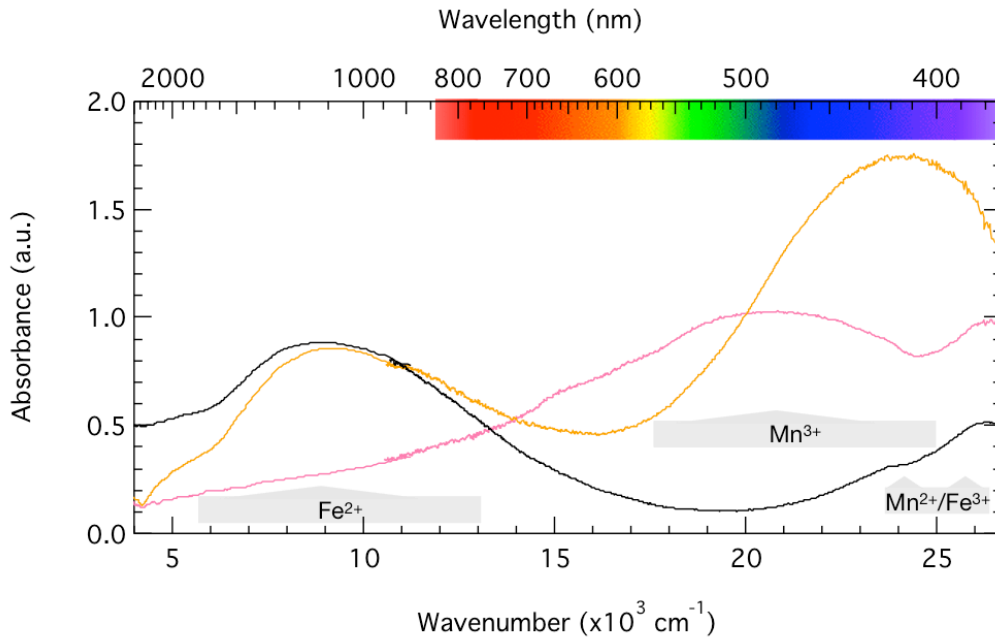
430
431
432 In the HCA approach we have included some minor elements. Are the clusters significant
433 regarding these components? Minor elements arising from raw material impurities might be
434 markers of distinct sources and may help to further distinguish or confirm the common origin of
435 glasses. Several authors have observed correlations between titanium and zirconium from heavy
436 minerals (Neri et al., 2019; Rehren and Brüggler, 2015; Schibille et al., 2016; Wedepohl et al.,
437 2011a) or strontium and rubidium from feldspars (Adlington and Freestone, 2017) and assigned
438 them to markers of the raw materials used for making the glass. Figure 5a and Figure 5b show
439 respectively the Ti and Zr and the Sr and Rb and Ba oxide contents. Cluster #1 forms a distinct
440 group regarding these five elements. Cluster #5 forms also a distinct group of glasses regarding
441 the Sr, Ba and Rb oxide contents. Clusters #2, #3 and #4 show similar Ti, Zr, Sr, Ba and Rb oxide
442 contents (Figure 5). Very close trace element contents may suggest a common glasshouse origin.
443 Yet the cluster #4 is quite distinct in terms of sodium oxide and magnesia contents. This
444 observation shines light on the difficulty to distinguish origins based on chemical composition:
445 bundles of glasses with similar trace element contents could be fortuitous, while important
446 variations in major elements could arise from a recipe variation in the glasshouse.
447 Although, the definition of the clusters is dependent on the method used (see SI), we have shown
448 that we can build significantly large clusters of glasses with low variability of major element
449 composition and corresponding to distinct trace element compositions. It suggests that these sub-
450 groups of glasses could, for most of the assigned samples, correspond to distinct bundles of
451 glasses.
452
453

454

3.4. Origin of the colors

455

3.4.1. Colorless, purple and yellow glasses



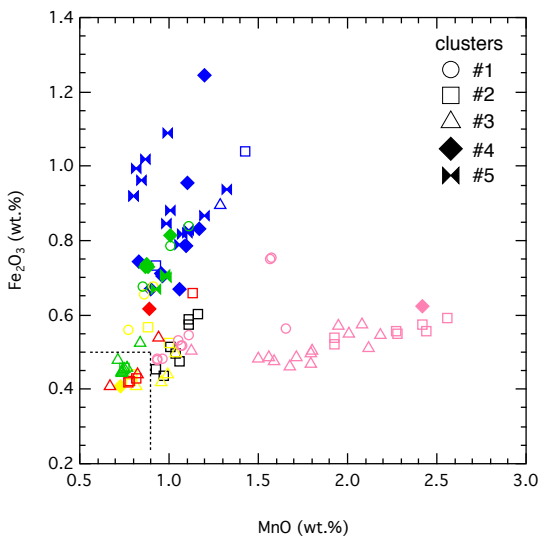
456

457

458

Figure 6: Optical absorption spectra of typical colorless, purple, and yellow glasses (with respective line color: pink, black and yellow) and assignment of the absorption bands.

459



460

461

462

463

Figure 7: Iron vs. manganese concentrations as total oxides with highlight on the colorless, purple and yellow glasses. Markers correspond to the clusters, color of the markers indicates the glass color, error bars are of the size of the markers.

464

465

466

467

468

469

470

471

We first consider the colorless, purple and yellow glasses. The optical absorption spectra (Figure 6) correspond to glass samples assigned to cluster #2. The absorption bands are identified and reveal that these glasses are all colored (or uncolored) by their respective iron and manganese contents (Table II) and corresponding redox states ($\text{Fe}^{2+}/\text{Fe}^{3+}$ and $\text{Mn}^{2+}/\text{Mn}^{3+}$). These three colors represent roughly only one third of the glazed surface (Figure 2b). This agrees with the relative difficulty and uncertainty to obtain these colors (Royce-Roll, 1994;

472 Schreurs and Brill, 1984; Sellner et al., 1979), which mainly result from a subtle balance between
473 the Fe/Mn ratio and the $\text{Fe}^{2+}/\text{Fe}^{3+}$ and $\text{Mn}^{2+}/\text{Mn}^{3+}$ relative amounts during glassmaking.

474

475 **Table II: Average iron and manganese contents (in wt.% \pm standard deviation) of the**
476 **colorless, purple and yellow glasses, independently of the cluster.**

Color	Fe_2O_3	MnO
Colorless	0.52 ± 0.06	1.0 ± 0.08
Purple	0.53 ± 0.07	1.65 ± 0.5
Yellow	0.50 ± 0.10	0.87 ± 0.1

477

478

- Colorless glass

479

480

481

482

483

484

485

486

487

488

489

490

491

492

493

494

495

496

497

498

499

500

501

502

503

504

- Purple glass

505

506

507

508

509

510

511

512

513

514

515

516

517

518

519

520

521

In the panels, colorless glasses are used for character's faces, walls, water, and folds. Colorless glasses correspond to glasses with no strong perceptible color hue, which translates in terms of CIE $L^*a^*b^*$ color coordinates as a^* and b^* being close to the center of the diagram ($a^*=0$ and $b^*=0$) and often the luminance L^* being higher than 50 (Figure 2c). These values agrees with other reported values for colorless glasses. (Bidegaray et al., 2020, 2019; Capobianco et al., 2019) Yet they show a greenish color (negative CIE a^*). The optical absorption spectrum of a typical colorless glass (Figure 6) from the Sainte-Chapelle in Paris agrees with previously published data. (Bidegaray et al., 2020, 2019; Capobianco et al., 2019; Hunault et al., 2017a) The greenish color is due to Fe^{2+} that gives a broad absorption band in the NIR centered at 9000cm^{-1} (1100nm) (Figure 6) and absorbs the red, orange and yellow wavelengths more than the green and blue side of the light spectrum. In glass, iron is present as Fe^{2+} and Fe^{3+} in various relative amounts depending on the glass chemical composition and redox conditions of fabrication. To remove the green color, the most common process is to oxidize Fe^{2+} into Fe^{3+} by adding an oxidizer to the glass, such as manganese and antimony. Red, yellow and some green glasses show the lowest iron and manganese contents (Figure 7), which allows us to define the impurity level concentrations to $<0.5\text{wt.}\%$ as total Fe_2O_3 for iron and to $<0.9\text{wt.}\%$ as total MnO for manganese (dashed lines in Figure 7). In Antiquity and the middle ages, glassmakers were using manganese in an oxidized form, referred to as "glassmaker's soap". (Bidegaray et al., 2020; Bingham and Jackson, 2008; Gliozzo, 2016; Jackson, 2005) The use of antimony in the glasses of this study is dismissed by the very low concentrations found in these glasses (maximum 200ppm). The colorless glasses of the Sainte-Chapelle in Paris, all belong to cluster #2 (Figure S7), and their manganese content is systematically larger than the impurity level concentrations (Figure 7 and Table II), which suggests the use of the "glassmakers' soap".

The optical absorption spectrum of purple glass from the Sainte-Chapelle agrees with typical spectra from Mn^{3+} colored glass. (Bidegaray et al., 2019; Capobianco et al., 2019; Hunault et al., 2017a). Compared to the colourless glasses, we observe the disappearance of the absorption band of Fe^{2+} , and the presence of Fe^{3+} and Mn^{2+} , which only give weak absorption bands in the blue and UV range (Figure 6). The addition of more oxidized manganese than iron results in all Fe^{2+} being oxidized (Schreiber, 1986). The excess of Mn^{3+} colors the glass in purple with a broad and intense absorption band around 20800cm^{-1} (480nm) (Figure 6). The color shift from colorless towards purplish hue is observed in the CIE $L^*a^*b^*$ diagram with a change from negative to positive a^* parameter. The purple glasses exhibit a large variation in the luminance values, with some strongly absorbing glass pieces (low L^* value). Visually, we observe two main uses of purple glass: characters' complexion using light purple or colorless glass and robes and dresses using more intense or darker purple glass. Figure 7 reveals two groups of purple glasses according to their Mn content: a first group with Mn content close to the impurity level and a second group with a clear increase of the total manganese content larger than the other colors ($>1.5\text{wt.}\%$), while the iron content remains mainly constant around $0.5\text{wt.}\%$ (Table II). We observe that all dark purple glasses have high manganese contents.

522
523
524
525
526
527
528
529
530
531
532
533
534
535
536
537
538
539
540
541
542
543
544
545
546
547
548
549
550
551

- Yellow glass

Yellow glasses were used for clothes, horns, and crowns. The CIE L*a*b* colorimetric coordinates spread in luminance L* and along the b* (yellow) direction as a* remains small and positive. They are bulk colored and show an optical absorption spectrum (Figure 6) with a broad absorption band centered at 9000cm⁻¹ (1100nm) assigned to the presence of Fe²⁺ as in the colorless glasses. An additional intense band in the UV creates the absorption deep centered ca. 16000cm⁻¹ (625nm) resulting in the yellow color. The lack of efficiency of the optical spectrometer source at high energy is responsible for the drop of absorption in the UV range in the recorded data. The addition of a complementary UV light source can improve the sensitivity in this energy range of the spectrum(Capobianco et al., 2019). The observed spectra differ from the yellow glasses of the rose of the cathedral of Reims (France) in the relatively more intense Fe²⁺ absorption band. (Capobianco et al., 2019) The bulk coloring, the dating of the glass and the optical absorption spectrum altogether converge with the exclusion of the use of yellow silver stain, a painting technique that appeared only at the end of the 13th century or at the very beginning of the 14th century.(Jembrih-Simbürger et al., 2002; Lautier and Sandron, 2008; Molina et al., 2013; Pérez-Villar et al., 2008) The chemical composition of the yellow glasses is close to that of the colorless glasses and prevents us from identifying without any ambiguity a specific coloring element. According to Figure 7, iron and manganese contents are among the lowest. There are little data in the literature about bulk medieval yellow glasses. The optical absorption spectrum is consistent with the coloring species being the ferric iron-sulfide chromophore similarly to amber glasses. Yet, the sulfur content does not show any significant pattern in relation with the yellow color (Figure S12). Specific reducing conditions as encountered in the elaboration of amber glasses could explain how such colors were obtained.(Paynter and Jackson, 2018; Schreurs and Brill, 1984) In his treatise, Theophilus' description of the making of yellow glass seems rather circumstantial.(Hawthorne and Smith, 1979) More detailed information can be found in the 18th century treatise of Georges Bontemps (Bontemps, 1868) who provided two recipes for bulk colored yellow glasses based on: i) a particular balance between iron and manganese concentrations or ii) the use of wood still containing sap. Altogether, it suggests that the color is obtained by several steps of melting and refining.

552
553
554
555
556
557
558
559
560
561
562

3.4.2. Blue glasses

As illustrated with panel c13 from window B111 (Figure 8a), we can distinguish two types of blue glass: light blue glass, used for clothes, walls and dark blue glass used mainly for the sky or background. This distinction can be further confirmed in terms of colorimetry (Figure 8b): dark blue glass pieces show luminance L* values all smaller than 40, while light blue glass pieces spread over the entire luminance range. Both types can also be distinguished in terms of color hue: while all blue glasses have a negative b* value in agreement with the blueish hue, the light blue glasses have a negative a* value, showing a green contribution to the color, while the dark blue glasses have a positive a* value revealing the red component of the color hue.

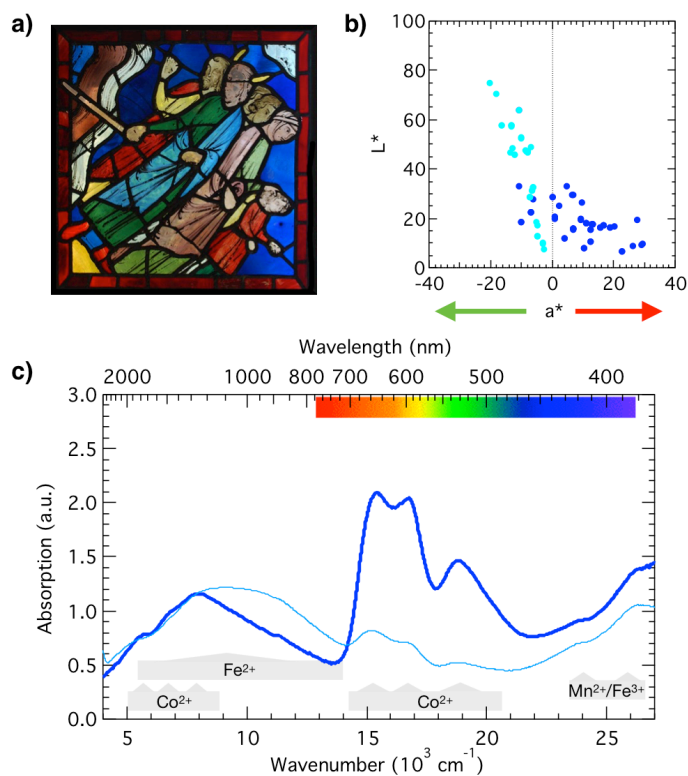


Figure 8: a) Panel c13 (w. 111) showing the two types of blue glass; b) Colorimetric parameters L^* vs. a^* ; c) Optical absorption spectra of typical dark blue glass and light blue glass and assignment of the absorption bands.

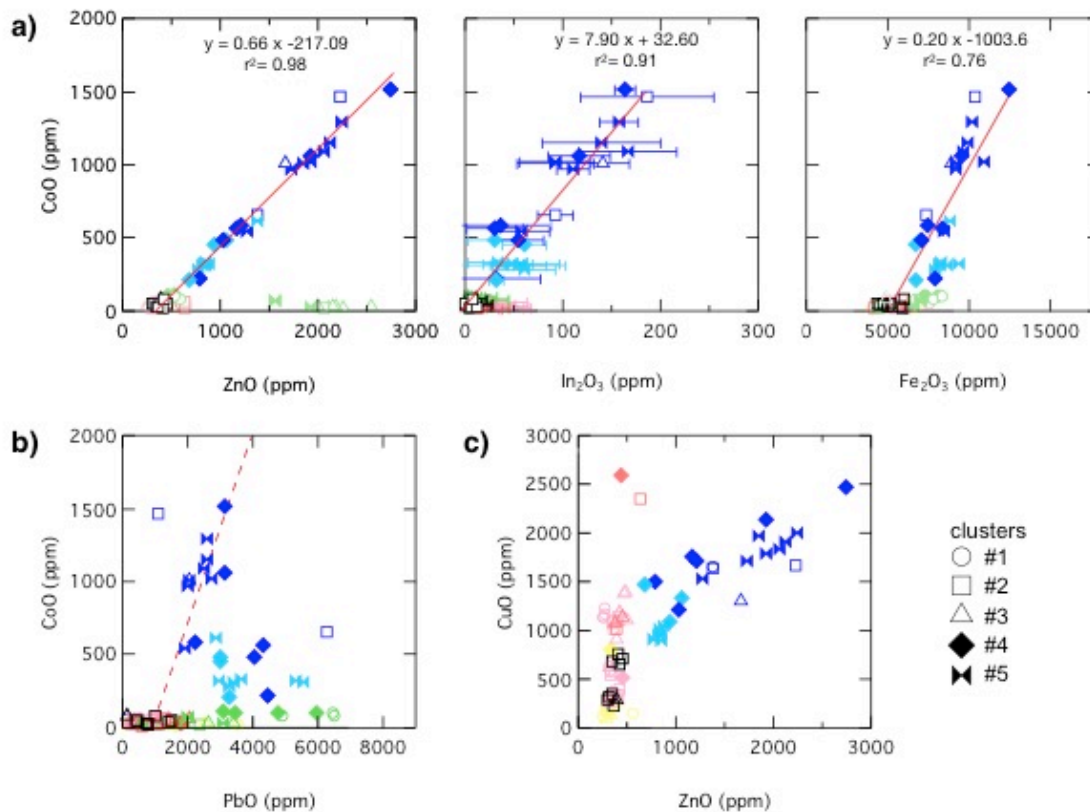
563
564
565

566

567 Figure 8c presents a selection of two optical absorption spectra representative of the two types
 568 of 13th century blue glasses of the Sainte-Chapelle in Paris: light blue and dark blue. We
 569 observe the contribution of the two triplet absorption bands in the NIR range at 5500-8000 cm⁻¹
 570 (1200-2000 nm) and the visible range at 15420, 16800 and 18800 cm⁻¹ (532, 595 and 650 nm)
 571 regions assigned to Co²⁺ (Bamford, 1977; Hunault et al., 2016a, 2014). These visible range
 572 bands are more intense for dark blue glass than light blue glass. The chemical composition
 573 analyses (Figure 9) confirm that Co²⁺ is the main coloring element in all blue glasses despite its
 574 relatively low concentration (maximum 1500ppm CoO). This is a result of its strong molar
 575 extinction coefficient. (Hunault et al., 2014). According to the Lambert-Beer law, the color
 576 intensity and darkness is proportional to the cobalt concentration assuming a constant glass
 577 thickness. Accordingly, we find that light blue glasses all correspond to low cobalt
 578 concentrations (Figure 9). The optical absorption spectra explain the color difference between
 579 the two types of blue: the Co²⁺ absorption bands are relatively narrow, resulting in sharp
 580 absorption of the yellow and green wavelengths, while the blue and red wavelengths are not
 581 absorbed thus resulting in a positive a^* parameter for dark blue glasses. In addition, we
 582 observe a broad absorption band between 7000 cm⁻¹ and 13000 cm⁻¹ (1428nm and 770nm)
 583 centered around 9000 cm⁻¹ (1100nm), superimposed on the near infrared absorption band of
 584 Co²⁺. We can attribute this contribution to Fe²⁺ similarly to the absorption band observed in the
 585 colorless glass. (Bingham and Jackson, 2008; Capobianco et al., 2019; Hunault et al., 2016a,
 586 2017a). The contribution from the Fe²⁺ band with respect to the Co²⁺ bands is higher in the light
 587 blue glasses. The overlap with the relatively intense Fe²⁺ absorption band results in a stronger
 588 absorption of the red wavelength and hence a dominant greenish-blueish hue (negative a^*).
 589 The small absorption bands around 24000 cm⁻¹ (417nm) attest for the presence of Mn²⁺ and
 590 Fe³⁺. (Nelson and White, 1980; Vercamer et al., 2015). No significant increase in the Mn content
 591 is observed (average MnO content in blue glasses: 0.96±0.40 wt.%) suggesting that manganese
 592 arises only from the raw materials used for the glass (Figure 7).

593

594
595



596
597
598
599
600
601

Figure 9: Chemical composition of the glasses obtained by PIXE at the new AGLAE facility in CoO v. a) ZnO, In_2O_3 , Fe_2O_3 and b) CuO v. ZnO and c) CoO v. PbO. Unless indicated, error bars are of the size of the markers. Redlines indicate the linear regression fitting of the data for ancient colorless and blue glasses only (other colors excluded from the fit). Equations of the lines are given. The dotted line corresponds to a slope of 0.66 in agreement with the chemical composition of saffre.

602
603
604
605
606
607
608
609
610
611
612
613
614
615
616
617
618
619
620
621
622
623
624
625
626

Blue glasses show clear correlations between cobalt and zinc and cobalt and indium contents (Figure 9a). These results agree with the sources of cobalt used in the 13th century: it has been demonstrated by previous works that from the 12th to the 13th century a change in the cobalt supply occurred and thus from the 13th century, cobalt was extracted from the Freiberg mines in Germany, characterized by the presence of specific trace elements: Zn, Pb and In. (Bidegaray and Pollard, 2018; Gratuze et al., 2018, 1995; Neri et al., 2019) No significant amounts of nickel are found (less than 50ppm, see SI) in agreement with the absence of Ni^{2+} absorption bands in the optical spectrum. (Galoisy et al., 2005)

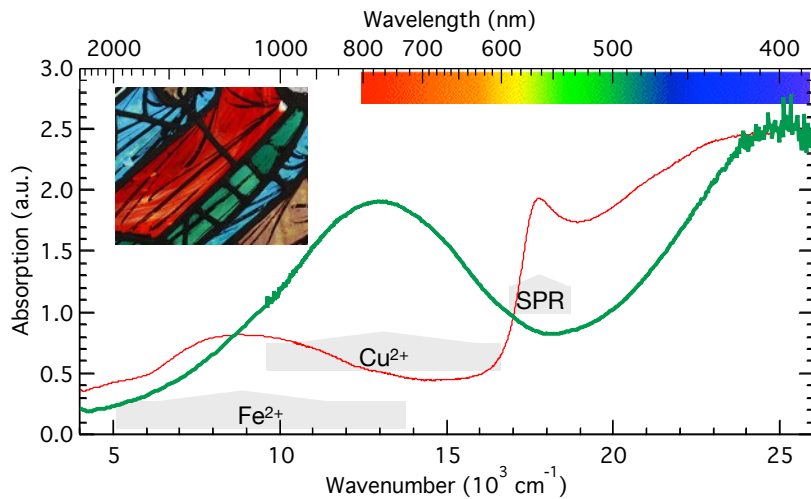
The mined cobalt was traded and probably added to the glass pot as *saffre*: a burnt cobalt ore mixed with sand. (Delamare, 2008; Gratuze et al., 2018) The composition of the *saffre* calculated from the analysis of ceramics decorations for the 13th-14th centuries period (Gratuze et al., 1996) suggests the following ratios between the mass compositions: $m(\text{CoO}) / m(\text{ZnO}) = m(\text{CoO}) / m(\text{PbO}) = 0.66$, $m(\text{CoO}) / m(\text{Fe}_2\text{O}_3) = 0.2$; $m(\text{CoO}) / m(\text{In}_2\text{O}_3) = 10.2$. The results of the linear regression fitting of the composition data from the blue glasses and colorless glasses are given in Figure 9 and agree with the calculated concentration ratios according to the estimated composition of *saffre*. These strong correlations across all samples of blue glass suggest the use of the same cobalt source for all of them. We note however that although the slope of the linear correlation between the iron and cobalt contents agrees with the *saffre* composition, the correlation factor is rather low. This might be explained by the fact that iron is also an important impurity from other raw materials and as a result strong variations arise from the raw materials. The relation between cobalt and lead contents does not show a clear correlation either, compared with the expected *saffre* composition (the expected relation is plotted in Figure 9b with a dashed line). In particular, we observe that for light blue glasses, the lead to cobalt ratio is larger than the ratio found in *saffre*.

627 Copper is another blue colorant of blue glass. In the present case, we demonstrate that copper is
628 not playing any role as blue colorant in these glasses and is an impurity associated to Zn. The
629 chemical composition of the blue glasses indicates that the Cu content varies between 0.1-
630 0.2wt.%. Copper can be present in the glass in 3 different oxidation states: Cu^0 , forming metallic
631 nano-particles (Kunicki-Goldfinger et al., 2014) (see the red glass section), Cu^+ which is colorless
632 (Hunault et al., 2016a, 2017a) and Cu^{2+} which gives a blueish or greenish hue.(Hunault and Loisel,
633 2020) The possible contribution of Cu^{2+} absorption, which is expected around 13000cm^{-1} (see
634 green glass section), is difficult to assess since it overlaps with Fe^{2+} (Figure 8c). According to
635 previous studies,(Hunault et al., 2016a) the redox conditions of blue medieval glasses favor Cu^+
636 oxidation state and a negligible contribution of Cu^{2+} . Therefore, the presence of copper in the
637 blue glasses is likely not directly related to the color. We observe some correlation between Cu
638 and Zn in blue glasses (Figure 9c) suggesting that both elements might be bound to the same
639 origin. Although the association of zinc with cobalt has been well described,(Gratuze et al., 2018,
640 1995) the origin of these impurities has been less discussed. So far, copper was not identified as a
641 significant impurity from the cobalt source along with zinc. Here, the association of copper and zinc
642 suggests a common source, for instance as brass. Hence, we could hypothesize that copper and
643 zinc co-occur with cobalt either as impurities from the original ore or as impurities coming from
644 brass tools used in the *saffre* elaboration process.
645

646 Most blue glasses belong either to clusters #4 or #5. They are characterized by a relatively high
647 sodium content compared to the other glasses (Figure 4b). However, the absence of any
648 significant correlation between the Na and Co contents prevents us from concluding on a relation
649 between the additions of these elements. This supports that, as mentioned above, the sodium-
650 enriched glasses are not specifically blue glasses and the presence of glasses of similar sodium
651 content but of different colors in the Sainte-Chapelle in Paris. Regarding the cobalt source, we
652 cannot distinguish between the two clusters. Furthermore the two ancient blue glasses with the
653 lowest sodium content (clusters #2 and #3) follow the same *saffre* impurity content. This suggests
654 that, if different, the glasshouses that produced these blue glasses used the same cobalt supply
655 from Germany. This would thus suggest that either these glasshouses were geographically close
656 or that the German provider had a monopoly of supply over a large region of France.
657

658 3.4.3. Green glasses

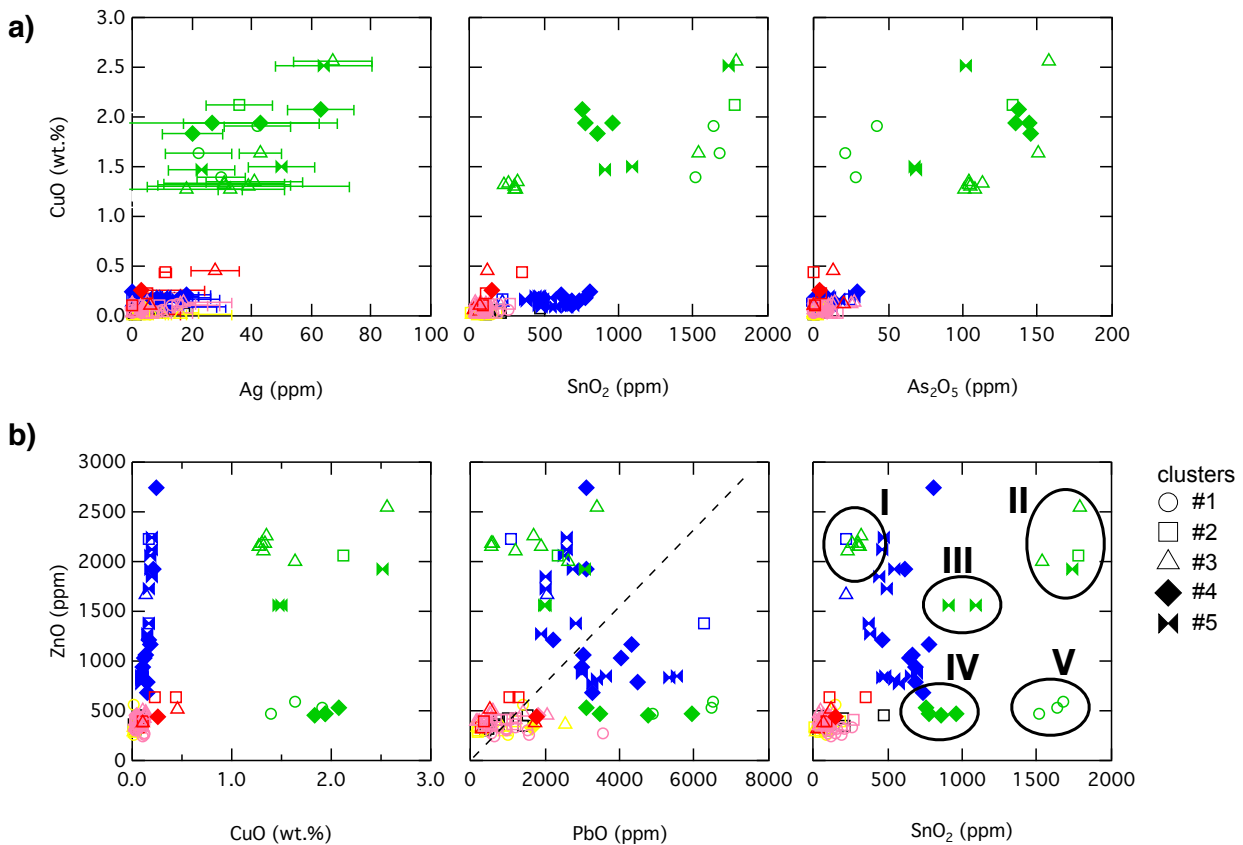
659 Green glass was mainly used for clothes and in fewer cases for the walls of buildings, trees, or
660 shoes. All ancient green glasses show similar optical absorption spectra (Figure 10) with a
661 characteristic absorption band from divalent copper ions centered at 13000cm^{-1} (770nm),
662 corresponding to the absorption of red wavelengths. This assignment agrees with the high
663 concentration of copper found in the green glasses (between 1.5-2 wt.% of total CuO) (Figure
664 10). Although Cu^{2+} alone gives a blue color to glass,(Bamford, 1977; Hunault and Loisel, 2020;
665 Smirniou and Rehren, 2013) the combination with the absorption of the blue wavelengths
666 revealed by the optical spectrum results creates a light transmission window in the green
667 around 18000cm^{-1} (550nm). The high energy absorption is assigned to Fe^{3+} .(Hunault and
668 Loisel, 2020) Compared to blue glasses, the absorption from Fe^{3+} is more intense. This is
669 assigned to the higher Fe^{3+} concentration in green glass in agreement with the redox
670 interaction between iron and copper. Indeed, high copper concentration is necessary to oxidize
671 completely all iron in the green glass such as it remains an excess of Cu^{2+} to color the glass.
672



673
674
675

Figure 10: Optical absorption spectra of green and red glasses with the corresponding assignment of the features. Inset: Detail of a panel showing the red and green glasses;

676



677
678
679

Figure 11: Chemical composition of the glasses obtained by PIXE at the New AGLAE facility a) Copper vs. silver, tin and arsenic contents; b) Zinc vs copper, lead and tin contents. Unless indicated, the error bars are of the size of the markers.

680

681 The use of copper to color glass in green is confirmed by the ancient treatises of Eraclius and
 682 Neri.(Vassas, 1971) Both texts report the use of calcined brass (copper-zinc alloy). It is of
 683 interest to compare the concentration of trace elements (Figure 11) in light of the clusters
 684 identified according to the glass matrix. Silver, tin and zinc, present as Ag^+ , Zn^{2+} and Sn^{4+}
 685 respectively, do not contribute to the color of the glass. Thus those elements are not added on
 686 purpose for the color but are likely brought by the copper source. In the Sn_2O -ZnO graph, we
 687 can distinguish five groups of green glasses. These groups fairly agree with the clusters
 688 defined by HCA according to the glass matrix. We find that the co-occurrence of copper and

689 silver, zinc and arsenic at higher concentrations than in colorless glasses for green glasses
690 from clusters #2, #3 and #5. However, green glasses from clusters #1 and #4 show low zinc
691 content similar to colorless glasses, ruling out the use of brass in favor of another copper alloy.
692 Green glasses from cluster #1 contain high tin content suggesting the use of a bronze alloy.
693 The presence of up to 60ppm of Ag in the green glasses suggests that the copper arises from
694 silver mines.(Bourgarit and Thomas, 2012; Craddock, 1985) Lead, another element part of the
695 copper metallurgy, is also found in significant amounts in green glasses (Figure 11b). It is anti-
696 correlated with the zinc content, forming two distinct groups: low zinc-high lead and high lead-
697 low zinc. It is the zinc-tin oxide binary plot that most clearly presents distinct groups of glasses:
698 we can define five groups of green glasses that have specific glass matrix compositions and
699 trace element contents (labeled from I to V in Figure 11b). Altogether we find that the green
700 glasses are marked by significantly different trace element contents. However, these groups do
701 not correlate with a particular panel or window but correspond to glasses from different panels
702 and different windows. This suggests that the four windows were glazed simultaneously using
703 the same glass stock supporting the existence of a large glazing atelier where an important
704 number of workers were collaborating.

705 3.4.4. Red glasses

706 In the studied windows, red glass was used for the branches and leaves of trees, clothes and
707 boots and for ornamental edges of the panels. All red glasses show a heterogeneous flame-like
708 pattern (Figure 10) that is called striated or “feuilleté”.(Kunicki-Goldfinger et al., 2014) This
709 technique was used from the 12th to the 14th century. Another technique for making red glass is
710 called “plaqué”: a flashed glass consisting in a thin layer of red on a thick layer of supporting
711 colorless glass. The latter was not found among the stained glass of the Sainte-Chapelle in
712 Paris. Both glass manufacturing techniques have one common goal: allowing red glass to be
713 translucent. Indeed, the red glasses show the characteristic absorption band of the surface
714 plasmon resonance (SPR) at 17800cm^{-1} (562nm) (Figure 10). The SPR is assigned to metallic
715 copper nanoparticles. The average size of the nanoparticles can be derived from the shape of the
716 plasmon resonance, using the equation $R = V_f \lambda_p^2 / (2\pi c \Delta\lambda)$, where R is the average radius of the
717 metallic nanoparticles, V_f is the Fermi velocity of the electrons in bulk metal (for Cu, $V_f = 15.7 \times 10^5$
718 cm s^{-1})(Kaye and Laby, 1948), λ_p is the peak position wavelength of the resonance, $\Delta\lambda$ is the full
719 width at half-maximum of the absorption band (here 20 nm), and c is the speed of light. This
720 equation predicts that the average size of Cu nanoparticles should be around 15 nm, in agreement
721 with the transmission electron microscope (TEM) observations from Kunicki et al.(Kunicki-
722 Goldfinger et al., 2014)

723 The absorption from the SPR is intense and therefore the making of translucent red glasses
724 requires a low concentration of nanoparticles or the elaboration of thin layers. Because of this
725 strong light absorption, the luminance L^* is lower than 50 for most red glasses (Figure 2). The
726 optical absorption spectrum also shows the absorption band of Fe^{2+} centered near 9000cm^{-1}
727 (1100nm).

728 Compared to the green glasses, in most red glasses the measured concentration is as low as
729 in colorless glasses (Figure 11), except two glasses reaching a maximum of 4500ppm. This
730 value is lower than the concentration in other studies.(Hunault et al., 2017a; Kunicki-Goldfinger
731 et al., 2014) The impossibility to detect significantly high Cu concentrations likely results from
732 the complex layered microstructure of the type-A “feuilleté” glasses (Kunicki-Goldfinger et al.,
733 2014) compared to the PIXE probing depth: the concentration determined by PIXE is an
734 average over both the colorless and the red layers. The chemical composition of the red layer
735 that could be probed does not reveal any specific presence of reducing species in agreement
736 with the fabrication process of Type-A red glasses. Eventually, we note that the red glasses
737 from the Sainte-Chapelle in Paris have a low CaO content similarly to most of the “Type-A”
738 glasses reported by Kunicki et al.(Kunicki-Goldfinger et al., 2014). All these glasses belong to
739 the same medieval period, the 12 and 13th centuries.

740

741 4. Conclusions

742
743 The restoration of the windows of the nave of the Sainte-Chapelle in Paris was a unique
744 opportunity to perform an in depth investigation of the chemistry and color of these glasses. With
745 105 glasses analyzed, we report the first extensive investigation of the links between chemistry
746 and color of Thirteenth Century glasses from the Saint-Chapelle in Paris. These data were
747 obtained using a combination of non-destructive techniques: PIXE-PIGE provides access to a wide
748 range of chemical elements, and optical absorption spectroscopy determines the nature of the
749 coloring species. Our results significantly complete the few other dataset already
750 published.(Lagabrielle and Velde, 2005; Verita et al., 2005)

751
752 The conclusions can be further summarized as follows:

- 753 - All ancient glasses have a potash-type chemical composition arising from a wood-ash glass
754 recipe in agreement with ancient medieval glassmaking treatises. The concentrations of major
755 and minor elements suggest the use of beech and bracken ashes.
- 756 - Hierarchical cluster analysis (HCA) allowed to define clusters of glasses of distinct glass matrix
757 chemical compositions. The low composition variability within each cluster, suggests that it
758 corresponds to a distinct bundle of glass. The chromophores and related impurities for a given
759 color form various sub-groups, which often correlate with the clusters, supporting that glasses
760 within a cluster originate from the same glasshouse. Whether or not these different bundles
761 originate from the same glasshouse is still difficult to confirm yet cannot be ruled out.
- 762 - A distinct compositional sub-group of glasses shows enriched sodium content. All but a few of
763 these glasses are blue glasses. The origin of the sodium remains unclear but might indicate a
764 distinct glasshouse origin, in Normandy, France. However, the fact that this characteristic
765 composition pattern is found in other windows in other colors supports that this is not specific to
766 the production of blue glasses and that the entire glazing project, although achieved by different
767 ateliers (glaziers), was supported by a unique glass supply.
- 768 - Colorless, purple and yellow colors arise from a subtle mastering of the manganese and iron
769 redox ratios.
- 770 - Blue glasses form two distinct color-hue groups: dark blue glasses are colored by cobalt and
771 light blue glasses are colored by lower cobalt contents and reduced iron. In all cases, Co, Zn
772 and In contents are correlated suggesting the use of *saffre* from the German mines of Freiberg.
773 The blue glasses are mainly split into two chemical composition clusters but the Co source
774 impurities follow a unique correlation suggesting that both sub-groups of blue glasses could
775 originate from the same glasshouse. It could alternatively imply that different glasshouses used
776 the same cobalt source and would confirm the monopoly of Germany as a cobalt supplier during
777 the 13th century.
- 778 - Green glasses are colored by divalent copper. The impurities arising from the copper source
779 enable to distinguish bundles of glass that fairly agree with the HCA clusters. This further
780 supports that the clusters correspond to bundles of glass that were used to glaze the different
781 windows simultaneously.
- 782 - Red glasses are “striated” glasses colored by metallic copper nanoparticles as observed in the
783 12th-13th centuries.
- 784 - Former painting style analyses published by art historians, suggest that the same atelier glazed
785 the four northern windows.(Grodecki and Brisac, 1984) The clusters and sub-groups of glasses
786 are not specific to a panel or a window, which confirms that the glazing work of at least these
787 four windows was conducted in parallel.

788
789 Altogether, the obtained chemical data overcome the lack of historiography and provide substantial
790 additional evidences of the organization of the glazing process conducted in a record time of a few
791 years: the glazing work of all the windows of the nave, although achieved probably by the
792 cooperation of several ateliers, used a common glass supply.

793

794 Other analytical techniques like electron micro-probe analysis (EMPA) or LA-ICP-MS could provide
795 additional compositional information on trace elements such as rare-earth, already used for
796 determining the origin of ancient glasses.(Wedepohl et al., 2011a, 2011b) However, this method
797 requires the sampling of the glasses. Even if this could be considered to some extent, then only a
798 restrained number of glasses would be selected to allow sampling the edge of the glass piece for
799 instance. Hence sampling a glass piece from the center of the panel would require dismantling the
800 panel or process to a very delicate endeavor of extracting one specific glass piece. Anyway, such
801 procedure would not allow the access to a large number of glasses as it has been done in the
802 present study thanks to the non-invasive IBA techniques at the New AGLAE facility.
803

804 Further investigations are required to provide a complete archaeological significance to the
805 chemical composition data. Comparison of these results with those of other contemporary
806 buildings should allow to complete our understanding of the history of medieval art and stained
807 glasses across France: trades of materials, sharing of knowledge and evolution of techniques,
808 which are already acknowledged in the studies of the art historians for the inventory of stained
809 glass. In particular, further studies on the chemical composition variations within glasshouses as
810 found in excavations in combination with investigations of the influence of the raw materials would
811 complete with quantitative definitions what Jackson et al.(Jackson et al., 2005) had defined earlier
812 as the “natural” and “behavioral” variability.
813
814
815

816

817 **Acknowledgements**

818

819 This work was supported by the Convergence project “VITRAUX” (SU-14-R-ScPC-15-2) from
820 Sorbonne Universités. The IBA analyses were performed at the New AGLAE facility (ANR-10-
821 EQPX-22). The authors thank Isabelle Pallot-Frossard for her continuous support and interest in
822 this project. M.O.J.Y.H. thanks François Guilhem and Serge Cohen for precious advises in the data
823 analysis using R software. Finally, the authors gratefully thank the two anonymous reviewers who
824 helped improve and clarify this paper to a great extent.

825

826 **Supporting information**

827

828 Restoration charts; dendrograms obtained using R and analysis of the clusters; comparison with
829 previous data. Chemical composition raw data; R code used for interpretation.

830

831

832 **References**

- 833 Adlington, L.W., Freestone, I.C., 2017. Using handheld pXRF to study medieval stained glass: A
834 methodology using trace elements. *MRS Adv.* 2, 1785–1800.
835 <https://doi.org/10.1557/adv.2017.233>
- 836 Adlington, L.W., Freestone, I.C., Kunicki-Goldfinger, J.J., Ayers, T., Gilderdale Scott, H., Eavis,
837 A., 2019. Regional patterns in medieval European glass composition as a provenancing tool.
838 *J. Archaeol. Sci.* 110, 104991. <https://doi.org/10.1016/j.jas.2019.104991>
- 839 Aubert, M., Grodecki, L., Lafond, J., Verrier, J., 1959. *Les Vitraux de Notre-Dame et de la Sainte-*
840 *Chapelle de Paris, Corpus vitrearum Medii Aevi. Caisse nationale des monuments*
841 *historiques Centre national de la recherche scientifique, Paris.*
- 842 Bamford, C.R., 1977. *Colour Generation and Control in Glass.* Elsevier Scientific Publishing
843 Company : distributors for the U.S. and Canada, Elsevier North-Holland.
- 844 Bidegaray, A.-I., Godet, S., Bogaerts, M., Cosyns, P., Nys, K., Terryn, H., Ceglia, A., 2019. To be
845 purple or not to be purple? How different production parameters influence colour and redox
846 in manganese containing glass. *J. Archaeol. Sci. Rep.* 27, 101975.
847 <https://doi.org/10.1016/j.jasrep.2019.101975>
- 848 Bidegaray, A.-I., Nys, K., Silvestri, A., Cosyns, P., Meulebroeck, W., Terryn, H., Godet, S., Ceglia,
849 A., 2020. 50 shades of colour: how thickness, iron redox and manganese/antimony contents
850 influence perceived and intrinsic colour in Roman glass. *Archaeol. Anthropol. Sci.* 12, 109.
851 <https://doi.org/10.1007/s12520-020-01050-0>
- 852 Bidegaray, A.-I., Pollard, A.M., 2018. Tesserae Recycling in the Production of Medieval Blue
853 Window Glass. *Archaeometry* 60, 784–796. <https://doi.org/10.1111/arc.12350>
- 854 Bingham, P.A., Jackson, C.M., 2008. Roman blue-green bottle glass: chemical–optical analysis and
855 high temperature viscosity modelling. *J. Archaeol. Sci.* 35, 302–309.
856 <https://doi.org/10.1016/j.jas.2007.03.011>
- 857 Bontemps, G., 1868. *Guide du verrier : traité historique et pratique de la fabrication des verres,*
858 *cristaux, vitraux / par G. Bontemps,... Librairie du “Dictionnaire des arts et manufactures”*
859 *(Paris).*
- 860 Bourgarit, D., Thomas, N., 2012. Late medieval copper alloying practices: a view from a Parisian
861 workshop of the 14th century AD. *J. Archaeol. Sci.* 39, 3052–3070.
862 <https://doi.org/10.1016/j.jas.2012.04.009>
- 863 Calligaro, T., 2008. PIXE in the study of archaeological and historical glass. *X-Ray Spectrom.* 37,
864 169–177. <https://doi.org/10.1002/xrs.1063>
- 865 Capobianco, N., Hunault, M.O.J.Y., Balcon-Berry, S., Galois, L., Sandron, D., Calas, G., 2019.
866 The Grande Rose of the Reims Cathedral: an eight-century perspective on the colour
867 management of medieval stained glass. *Sci. Rep.* 9, 3287. <https://doi.org/10.1038/s41598-019-39740-y>
- 869 Cox, G.A., Gillies, K.J.S., 1986. The X-Ray Fluorescence Analysis of Medieval Durable Blue Soda
870 Glass from York Minster. *Archaeometry* 28, 57–68. <https://doi.org/10.1111/j.1475-4754.1986.tb00374.x>
- 872 Craddock, P.T., 1985. Medieval Copper Alloy Production and West African Bronze Analyses - Part
873 I. *Archaeometry* 27, 17–41. <https://doi.org/10.1111/j.1475-4754.1985.tb00344.x>
- 874 Delamare, F., 2008. *Bleus en poudres: de l’art à l’industrie : 5000 ans d’innovations.* Presses des
875 MINES.
- 876 Fleming, S.J., Swann, C.P., 1987. Color additives and trace elements in ancient glasses: Specialized
877 studies using PIXE spectrometry. *Nuclear Instruments and Methods in Physics Research*
878 *Section B: Beam Interactions with Materials and Atoms* 22, 411–418.
879 [https://doi.org/10.1016/0168-583X\(87\)90368-5](https://doi.org/10.1016/0168-583X(87)90368-5)
- 880 Freestone, I., Price, J., Cartwright, C., 2009. The batch: its recognition and significance, in:
881 Janssens, K.H.A., *Congrès international d’étude historique du verre, International*
882 *Association for the History of Glass (Eds.), Annales Du 17e Congrès de l’Association*
883 *Internationale Pour l’Histoire Du Verre, Anvers, 2006 =: Annales of the 17th Congress of*

- 884 the International Association for the History of Glass, 2006, Antwerp. University Press
885 Antwerp, Antwerp, pp. 130–135.
- 886 Freestone, I.C., 1992. Theophilus and the Composition of Medieval Glass, in: Symposium J –
887 Materials Issues in Art and Archaeology III, MRS Online Proceedings Library.
888 <https://doi.org/10.1557/PROC-267-739>
- 889 Galoisy, L., Calas, G., Cormier, L., Marcq, B., Thibault, M.H., 2005. Overview of the environment
890 of Ni in oxide glasses in relation to the glass colouration. *Physics and Chemistry of Glasses*
891 46, 394–399.
- 892 Gliozzo, E., 2016. The composition of colourless glass: a review. *Archaeol. Anthropol. Sci.* 1–29.
893 <https://doi.org/10.1007/s12520-016-0388-y>
- 894 Gratuze, B., 2013. Provenance Analysis of Glass Artefacts, in: Janssens, K. (Ed.), *Modern Methods*
895 *for Analysing Archaeological and Historical Glass*. John Wiley & Sons Ltd, pp. 311–343.
- 896 Gratuze, B., Pactat, I., Schibille, N., 2018. Changes in the Signature of Cobalt Colorants in Late
897 Antique and Early Islamic Glass Production. *Minerals* 8, 225.
898 <https://doi.org/10.3390/min8060225>
- 899 Gratuze, B., Soulier, I., Barrandon, J.N., Foy, D., 1995. The origin of cobalt blue pigments in french
900 glass from the thirteenth to the eighteenth centuries. *Trade and discovery: the scientific*
901 *study of artefacts from post-medieval Europe and beyond* 123–33.
- 902 Gratuze, B., Soulier, I., Blet, M., Vallauri, L., 1996. De l'origine du cobalt: du verre à la céramique.
903 *Revue d'archéométrie* 77–94.
- 904 Grodecki, L., 1976. Le chapitre XXVIII de la *Schedula* du moine Théophile: technique et esthétique
905 du vitrail roman. *Comptes rendus des séances de l'Académie des Inscriptions et Belles-*
906 *Lettres* 120, 345–357. <https://doi.org/10.3406/crai.1976.13258>
- 907 Grodecki, L., Brisac, C., 1984. *Le vitrail gothique: au XIIIème siècle*. Vilo/office du livre.
- 908 Hawthorne, J.G., Smith, C.S., 1979. *Theophilus on Divers Arts: the foremost medieval treatise on*
909 *painting, glassmaking and metal-work*. Translated from the Latin with introduction and
910 notes, Dover Publications, Inc. ed. New York.
- 911 Hunault, M., Bauchau, F., Loisel, C., Hérold, M., Galoisy, L., Newville, M., Calas, G., 2016a.
912 Spectroscopic Investigation of the Coloration and Fabrication Conditions of Medieval Blue
913 Glasses. *J. Am. Ceram. Soc.* 99, 89–97. <https://doi.org/10.1111/jace.13783>
- 914 Hunault, M., Calas, G., Galoisy, L., Lelong, G., Newville, M., 2014. Local Ordering Around
915 Tetrahedral Co²⁺ in Silicate Glasses. *J. Am. Ceram. Soc.* 97, 60–62.
916 <https://doi.org/10.1111/jace.12709>
- 917 Hunault, M., Lelong, G., Gauthier, M., Gélébart, F., Ismael, S., Galoisy, L., Bauchau, F., Loisel, C.,
918 Calas, G., 2016b. Assessment of Transition Element Speciation in Glasses Using a Portable
919 Transmission Ultraviolet–Visible–Near-Infrared (UV-Vis-NIR) Spectrometer. *Appl*
920 *Spectrosc* 70, 778–784. <https://doi.org/10.1177/0003702816638236>
- 921 Hunault, M.O.J.Y., Loisel, C., 2020. Looking through model medieval green glasses: From color to
922 recipe. *International Journal of Applied Glass Science* 11, 463–470.
923 <https://doi.org/10.1111/ijag.15134>
- 924 Hunault, M.O.J.Y., Loisel, C., Bauchau, F., Lemasson, Q., Pacheco, C., Pichon, L., Moignard, B.,
925 Boulanger, K., Hérold, M., Calas, G., Pallot-Frossard, I., 2017a. Nondestructive Redox
926 Quantification Reveals Glassmaking of Rare French Gothic Stained Glasses. *Anal. Chem.*
927 <https://doi.org/10.1021/acs.analchem.7b01452>
- 928 Hunault, M.O.J.Y., Vinel, V., Cormier, L., Calas, G., 2017b. Thermodynamic insight into the
929 evolution of medieval glassworking properties. *J. Am. Ceram. Soc.* 89, 6277–6284.
930 <https://doi.org/10.1111/jace.14819>
- 931 Jackson, C.M., 2005. Making Colourless Glass in the Roman Period*. *Archaeometry* 47, 763–780.
932 <https://doi.org/10.1111/j.1475-4754.2005.00231.x>
- 933 Jackson, C.M., Booth, C.A., Smedley, J.W., 2005. Glass by design? Raw materials, recipes and
934 compositional data. *Archaeometry* 47, 781–795.

- 935 Jackson, C.M., Smedley, J.W., 2008. Medieval and post-medieval glass technology: seasonal
936 changes in the composition of bracken ashes from different habitats through a growing
937 season. *Glass Technology-European Journal of Glass Science and Technology Part A* 49,
938 240–245.
- 939 Jackson, C.M., Smedley, J.W., 2004. Medieval and post-medieval glass technology: melting
940 characteristics of some glasses melted from vegetable ash and sand mixtures. *Glass*
941 *Technol.: Eur. J. Glass Sci. Technol., Part A* 45, 36–42.
- 942 Jembrih-Simbürger, D., Neelmeijer, C., Schalm, O., Fredrickx, P., Schreiner, M., De Vis, K.,
943 Mäder, M., Schryvers, D., Caen, J., 2002. The colour of silver stained glass—analytical
944 investigations carried out with XRF, SEM/EDX, TEM, and IBA. *J. Anal. At. Spectrom.* 17,
945 321–328. <https://doi.org/10.1039/B111024C>
- 946 Kaye, G.W.C., Laby, T.H., 1948. Tables of physical and chemical constants and some mathematical
947 functions. London, Royaume-Uni de Grande-Bretagne et d'Irlande du Nord.
- 948 Kuisma-Kursula, P., 2000. Accuracy, precision and detection limits of SEM–WDS, SEM–EDS and
949 PIXE in the multi-elemental analysis of medieval glass. *X-Ray Spectrometry* 29, 111–118.
950 [https://doi.org/10.1002/\(SICI\)1097-4539\(200001/02\)29:1<111::AID-XRS408>3.0.CO;2-W](https://doi.org/10.1002/(SICI)1097-4539(200001/02)29:1<111::AID-XRS408>3.0.CO;2-W)
- 951 Kunicki-Goldfinger, J., Kierzek, J., Kasprzak, A., Małzewska-Bućko, B., 2000. A study of
952 eighteenth century glass vessels from central Europe by x-ray fluorescence analysis. *X-Ray*
953 *Spectrometry* 29, 310–316. [https://doi.org/10.1002/1097-4539\(200007/08\)29:4<310::AID-XRS431>3.0.CO;2-E](https://doi.org/10.1002/1097-4539(200007/08)29:4<310::AID-XRS431>3.0.CO;2-E)
- 954 Kunicki-Goldfinger, J.J., Freestone, I.C., McDonald, I., Hobot, J.A., Gilderdale-Scott, H., Ayers,
955 T., 2014. Technology, production and chronology of red window glass in the medieval
956 period – rediscovery of a lost technology. *J. Archaeol. Sci.* 41, 89–105.
957 <https://doi.org/10.1016/j.jas.2013.07.029>
- 958 Lagabrielle, S., Velde, B., 2005. Evolution of French stained glass compositions during the middle
959 Ages - Analyses and observations made on the Cluny collection, in: *Annales Du 16e*
960 *Congrès de l'Association Internationale Pour l'Histoire Du Verre.* pp. 341–346.
- 961 Lautier, C., Kurmann-Schwarz, B., 2010. Recherches récentes sur le vitrail médiéval, 1998-2009.
962 2e partie. *Kunstchronik* 63, 313–338.
- 963 Lautier, C., Sandron, D., 2008. Antoine de Pise: l'art du vitrail vers 1400. CTHS, Comité des
964 travaux historiques et scientifiques.
- 965 Loisel, C., 2020. La Sainte-Chapelle de Paris : Analyser et restaurer pour conserver ce joyau.
966 Beaux-Arts Editions 32–35.
- 967 Molina, G., Murcia, S., Molera, J., Roldan, C., Crespo, D., Pradell, T., 2013. Color and dichroism
968 of silver-stained glasses. *J Nanopart Res* 15, 1932. <https://doi.org/10.1007/s11051-013-1932-7>
- 969
970
- 971 Musso, P., 2017. La Religion industrielle: Monastère, manufacture, usine. Une généalogie de
972 l'entreprise, Fayard. ed. Paris, France.
- 973 Nelson, C., White, W., 1980. Transition metal ions in silicate melts—I. Manganese in sodium
974 silicate melts. *Geochim. Cosmochim. Acta* 44, 887–893. [https://doi.org/10.1016/0016-7037\(80\)90269-0](https://doi.org/10.1016/0016-7037(80)90269-0)
- 975
- 976 Neri, E., Gratuze, B., Schibille, N., 2019. The trade of glass beads in early medieval Illyricum:
977 towards an Islamic monopoly. *Archaeol. Anthropol. Sci.* 11, 1107–1122.
978 <https://doi.org/10.1007/s12520-017-0583-5>
- 979 Pallot-Frossard, I., 1998. La place du vitrail dans l'architecture ?, in: *Le Matériau Vitreux : Verre et*
980 *Vitraux / Actes Du Cours Intensif Européen, Ravello, 28-30 Avril 1995.* Bari : Edipuglia,
981 Centro universitario europeo per i beni culturali, Ravello, pp. 23–42.
- 982 Panofsky, E., 1946. Abbot Suger on the Abbey Church of St.-Denis and its art treasures. Princeton
983 University Press, Princeton (N.J.), Etats-Unis.
- 984 Paynter, S., Jackson, C.M., 2018. Mellow yellow: An experiment in amber. *J. Archaeol. Sci. Rep.*
985 22, 568–576. <https://doi.org/10.1016/j.jasrep.2017.11.038>

- 986 Pérez-Villar, S., Rubio, J., Oteo, J.L., 2008. Study of color and structural changes in silver painted
987 medieval glasses. *J. Non-Cryst. Solids* 354, 1833–1844.
988 <https://doi.org/10.1016/j.jnoncrysol.2007.10.008>
- 989 Phelps, M., Freestone, I.C., Gorin-Rosen, Y., Gratuze, B., 2016. Natron glass production and supply
990 in the late antique and early medieval Near East: The effect of the Byzantine-Islamic
991 transition. *J. Archaeol. Sci.* 75, 57–71. <https://doi.org/10.1016/j.jas.2016.08.006>
- 992 Pichon, L., Calligaro, T., Lemasson, Q., Moignard, B., Pacheco, C., 2015. Programs for
993 visualization, handling and quantification of PIXE maps at the AGLAE facility. *Nucl.*
994 *Instrum. Methods Phys. Res., Sect. B.* <https://doi.org/10.1016/j.nimb.2015.08.086>
- 995 Pichon, L., Moignard, B., Lemasson, Q., Pacheco, C., Walter, P., 2014. Development of a multi-
996 detector and a systematic imaging system on the AGLAE external beam. *Nucl. Instrum.*
997 *Methods Phys. Res., Sect. B* 318, 27–31. <https://doi.org/10.1016/j.nimb.2013.06.065>
- 998 Rehren, T., Brüggler, M., 2015. Composition and production of late antique glass bowls type Helle.
999 *J. Archaeol. Sci. Rep.* 3, 171–180. <https://doi.org/10.1016/j.jasrep.2015.05.021>
- 1000 Rehren, Th., Freestone, I.C., 2015. Ancient glass: from kaleidoscope to crystal ball. *J. Archaeol.*
1001 *Sci., Scoping the Future of Archaeological Science: Papers in Honour of Richard Klein* 56,
1002 233–241. <https://doi.org/10.1016/j.jas.2015.02.021>
- 1003 Royce-Roll, D., 1994. THE COLORS OF ROMANESQUE STAINED GLASS. *Journal of Glass*
1004 *Studies* 3, 71–80.
- 1005 Schalm, O., Caluwé, D., Wouters, H., Janssens, K., Verhaeghe, F., Pieters, M., 2004. Chemical
1006 composition and deterioration of glass excavated in the 15th–16th century fishermen town
1007 of Raversijde (Belgium). *Spectrochim. Acta, Part B* 59, 1647–1656.
1008 <https://doi.org/10.1016/j.sab.2004.07.012>
- 1009 Schalm, O., Janssens, K., Wouters, H., Caluwé, D., 2007. Composition of 12–18th century window
1010 glass in Belgium: Non-figurative windows in secular buildings and stained-glass windows in
1011 religious buildings. *Spectrochim. Acta, Part B* 62, 663–668.
1012 <https://doi.org/10.1016/j.sab.2007.03.006>
- 1013 Schibille, N., Meek, A., Tobias, B., Entwistle, C., Avisseau-Broustet, M., Da Mota, H., Gratuze, B.,
1014 2016. Comprehensive Chemical Characterisation of Byzantine Glass Weights. *PLoS ONE*
1015 11, e0168289. <https://doi.org/10.1371/journal.pone.0168289>
- 1016 Schreiber, H.D., 1986. Redox processes in glass-forming melts. *J. Non-Cryst. Solids* 84, 129–141.
- 1017 Schreurs, J.W.H., Brill, R.H., 1984. Iron and Sulfur Related Colors in Ancient Glasses.
1018 *Archaeometry* 26, 199–209. <https://doi.org/10.1111/j.1475-4754.1984.tb00334.x>
- 1019 Sellner, C., Oel, H., Camara, B., 1979. Untersuchung alter Gläser (Waldglas) auf Zusammenhang
1020 von Zusammensetzung, Farbe und Schmelzatmosfera mit der Elektronenspektroskopie und
1021 der Elektronenspinresonanz (ESR). *Glastechn. Ber.* 52, 255–264.
- 1022 Smedley, J.W., Jackson, C.M., 2002. Medieval and post-medieval glass technology: a review of
1023 bracken in glassmaking. *Glass Technology* 43, 221–224.
- 1024 Smedley, J.W., Jackson, C.M., Booth, C.A., 1998. BACK TO THE ROOTS : THE RAW
1025 MATERIALS, GLASS RECIPES AND GLASSMAKING PRACTICES OF
1026 THEOPHILUS, in: *Prehistory and History of Glassmaking Technology, Ceramics and*
1027 *Civilization. Presented at the 99th Annual meeting of the American Ceramic Society,*
1028 *American Ceramic Society, pp. 145–166.*
- 1029 Smirniou, M., Rehren, T., 2013. Shades of blue – cobalt-copper coloured blue glass from New
1030 Kingdom Egypt and the Mycenaean World: a matter of production or colorant source? *J.*
1031 *Archaeol. Sci.* 40, 4731–4743. <https://doi.org/10.1016/j.jas.2013.06.029>
- 1032 Smith, E.B., 2015. ‘All my stained glass which I brought from Europe’: William Poyntell and the
1033 Sainte-Chapelle medallions. *HISCOL* 27, 323–334. <https://doi.org/10.1093/jhc/fhu049>
- 1034 Stern, W.B., Gerber, Y., 2004. Potassium–Calcium Glass: New Data and Experiments*.
1035 *Archaeometry* 46, 137–156. <https://doi.org/10.1111/j.1475-4754.2004.00149.x>
- 1036 Theophilus, 1847. *Diversarum artium schedula.* J. Murray.

- 1037 Tite, M.S., Shortland, A., Maniatis, Y., Kavoussanaki, D., Harris, S.A., 2006. The composition of
1038 the soda-rich and mixed alkali plant ashes used in the production of glass. *J. Archaeol. Sci.*
1039 33, 1284–1292. <https://doi.org/10.1016/j.jas.2006.01.004>
- 1040 Van Wersch, L., Loisel, C., Mathis, F., Strivay, D., Bully, S., 2016. Analyses of Early Medieval
1041 Stained Window Glass From the Monastery of Baume-Les-Messieurs (Jura, France).
1042 *Archaeometry* 58, 930–946. <https://doi.org/10.1111/arc.12207>
- 1043 Vassas, C.D., 1971. Etude chimique, thermographique et physique de verres de vitraux du Moyen-
1044 Age, in: *Communications scientifiques et techniques*. Presented at the Congrès international
1045 du verre, Versailles, France.
- 1046 Vercamer, V., Lelong, G., Hijiya, H., Kondo, Y., Galois, L., Calas, G., 2015. Diluted Fe³⁺ in
1047 silicate glasses: Structural effects of Fe-redox state and matrix composition. An optical
1048 absorption and X-band/Q-band EPR study. *J. Non-Cryst. Solids* 428, 138–145.
1049 <https://doi.org/10.1016/j.jnoncrysol.2015.08.010>
- 1050 Verita, M., Nicola, C., Sommariva, G., 2005. The stained glass windows of the Sainte Chapelle in
1051 Paris: Investigations on the origin of the loss of the painted work, in: *Annales Du 16e*
1052 *Congrès de l'Association Internationale Pour l'Histoire Du Verre*. pp. 347–351.
- 1053 Vilarigues, M., Coutinho, I., Medici, T., Alves, L.C., Gratuze, B., Machado, A., 2019. From beams
1054 to glass: determining compositions to study provenance and production techniques. *Physical*
1055 *Sciences Reviews* 0. <https://doi.org/10.1515/psr-2018-0019>
- 1056 Vilarigues, M., da Silva, R.C., 2004. Ion beam and infrared analysis of medieval stained glass.
1057 *Appl. Phys. A* 79, 373–378. <https://doi.org/10.1007/s00339-004-2538-9>
- 1058 Wedepohl, K.H., Simon, K., 2010. The chemical composition of medieval wood ash glass from
1059 Central Europe. *Chemie der Erde - Geochemistry* 70, 89–97.
1060 <https://doi.org/10.1016/j.chemer.2009.12.006>
- 1061 Wedepohl, K.H., Simon, K., Kronz, A., 2011a. Data on 61 Chemical Elements for the
1062 Characterization of Three Major Glass Compositions in Late Antiquity and the Middle
1063 Ages. *Archaeometry* 53, 81–102. <https://doi.org/10.1111/j.1475-4754.2010.00536.x>
- 1064 Wedepohl, K.H., Simon, K., Kronz, A., 2011b. The chemical composition including the Rare Earth
1065 Elements of the three major glass types of Europe and the Orient used in late antiquity and
1066 the Middle Ages. *Geochemistry* 71, 289–296. <https://doi.org/10.1016/j.chemer.2011.04.001>
- 1067